AD-A072 749 STATE UNIV OF NEW YORK COLL OF ENVIRONMENTAL SCIENCE --ETC F/G 8/5
EXTENSION OF GROUND CONTROL WITH MOVING AIRBORNE TARGETS.(U)
JUN 79 D I ZULCH, R H BROCK F30602-75-C-0122

UNCLASSIFIED RADC-TR-79-169 NL

| OF |
AD
A072749

END
DATE
FILMED
9-79
DDC

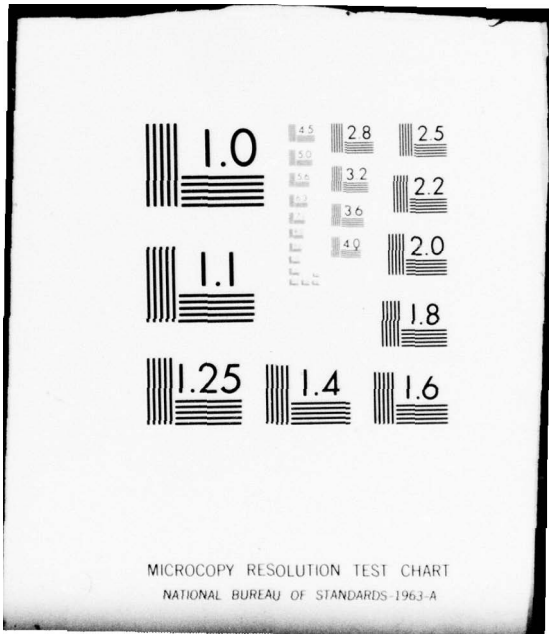
1.0
1.1
1.25
1.4
1.6
1.8
2.0
2.2
2.5
2.8
3.2
3.6
4.0
4.5
5.0
5.6
MICROCOPY RESOLUTION TEST CHART
NATIONAL BUREAU OF STANDARDS-1963-A

RADC-TR-79-169
In-House Report
June 1979

LEVEL II 12 B.S.

EXTENSION OF GROUND CONTROL WITH MOVING AIRBORNE TARGETS

Donald I. Zulch (RADC/DCI)
Robert H. Brock, Jr. (College of Environmental Science & Forestry)

ROME AIR DEVELOPMENT CENTER
Air Force Systems Command
Griffiss Air Force Base, New York 13441

This report has been reviewed by the RADC Information Office (OI) and is releasable to the National Technical Information Service (NTIS). At NTIS it will be releasable to the general public, including foreign nations.

RADC-TR-79-169 has been reviewed and is approved for publication.

APPROVED: John N. Entzminger Jr

JOHN N. ENTZMINGER, Jr.
Chief, Location & Control Brauch
Communications & Control Division

APPROVED: Fred I. Diamond

FRED I. DIAMOND
Technical Director
Communications & Control Division

FOR THE COMMANDER: John P. Huss

JOHN P. HUSS
Acting Chief, Plans Office

If your address has changed or if you wish to be removed from the RADC mailing list, or if the addressee is no longer employed by your organization, please notify RADC (DCI) Griffiss AFB NY 13441. This will assist us in maintaining a current mailing list.

Do not return this copy. Retain or destroy.

UNCLASSIFIED

SECURITY CLASSIFICATION OF THIS PAGE (When Data Entered)

REPORT DOCUMENTATION PAGE

READ INSTRUCTIONS BEFORE COMPLETING FORM

1. REPORT NUMBER: RADC-TR-79-169	2. GOVT ACCESSION NO.
3. RECIPIENT'S CATALOG NUMBER	
4. TITLE (and Subtitle): EXTENSION OF GROUND CONTROL WITH MOVING AIRBORNE TARGETS	5. TYPE OF REPORT & PERIOD COVERED: Final Technical Report. May 1977 - October 1978
6. PERFORMING ORG. REPORT NUMBER: N/A	
7. AUTHOR(s): Donald I. Zulch (RADC/DCI); Robert H. Brock, Jr. (College of Environmental Science & Forestry, Syracuse NY)	8. CONTRACT OR GRANT NUMBER(s): F30602-75-C-0122
9. PERFORMING ORGANIZATION NAME AND ADDRESS: Rome Air Development Center (DCI) Griffiss AFB NY 13441	10. PROGRAM ELEMENT, PROJECT, TASK AREA & WORK UNIT NUMBERS: P.E. 63747F; P.E. 62702F; J.O. 221701P0
11. CONTROLLING OFFICE NAME AND ADDRESS: Rome Air Development Center (DCI) Griffiss AFB NY 13441	12. REPORT DATE: June 1979; 13. NUMBER OF PAGES
14. MONITORING AGENCY NAME & ADDRESS (if different from Controlling Office): Same	15. SECURITY CLASS. (of this report): UNCLASSIFIED; 15a. DECLASSIFICATION/DOWNGRADING SCHEDULE: N/A

16. DISTRIBUTION STATEMENT (of this Report)

Approved for public release; distribution unlimited.

16 2217 17 01

17. DISTRIBUTION STATEMENT (of the abstract entered in Block 20, if different from Report)

Same

18. SUPPLEMENTARY NOTES

This report is a combined RADC/contractor report with both authors contributing.

19. KEY WORDS (Continue on reverse side if necessary and identify by block number)

Photogrammetry	Geodetic
Aerotriangulation	Geodetic Control
DME Navigation	Geodetic Control Extension

20. ABSTRACT (Continue on reverse side if necessary and identify by block number)

A method of extending geodetic control to geographical areas in which control is sparse or nonexistent makes use of unique combination of aerotriangulation and distance measuring technology. Aircraft or drones are flown over a designated area under control of a radial electronic navigation system. A second higher flying aircraft containing an accurately calibrated metric camera is controlled over the same area and aerial photographs are taken in sequence. Imagery includes both lower flying aircraft and area in which control is desired. Both camera, imagery and photographed aircraft are in a common

DD FORM 1 JAN 73 1473

UNCLASSIFIED

SECURITY CLASSIFICATION OF THIS PAGE (When Data Entered)

State Univ of New York
Coll. of Env. Sci. & Forestry, Syracuse 33950

highly accurate coordinate system. A detailed error analysis was conducted using four aircraft and four ground beacons. The ground beacons are geodetic anchors for the distance measuring equipment navigation system (DME). Ground surveys of existing DME navigation range at RADC were used. Equipment errors from actual equipment were used. Standard corrections for environmental effects were made. The concept was as good as the standard ground techniques for ground control extension. The moving target technique is flexible and aircraft can be commanded to take advantage of lines of flight providing the superior geometry and smallest errors in X, Y and Z coordinates. The use of aero-triangulation and DME navigation represents an order of magnitude decrease in the time required to perform conventional surveys to DME navigation system requirements.

TABLE OF CONTENTS

		Page
1.0	Introduction	1
	1.1 Background	1
	1.2 General System Concept and Purpose of Investigation	3
2.0	Investigation of Combined DME and Aerial Photography for Ground Control Extension	8
	2.1 General	8
	2.2 Instrumentation Range and Survey Control	8
	2.3 Distance Measurement and Survey Errors	9
	2.4 High Altitude Photography	19
	2.5 Analytic Aerotriangulation	19
	2.6 Results	24
3.0	Discussion of Results	32
4.0	Conclusions and Recommendations	37
5.0	References	38
	Appendix A - Distance Measurement Equipment Navigation	A-1
	Appendix B - General Photogrammetric Bundle Adjustment Solution	B-1

1.0 INTRODUCTION

1.1 BACKGROUND

The subject of extending survey control into unchartered areas has been of interest for many years. The AN/USQ 28 system was one of the more well known systems.[1] As progress in mapping continues the efficiency of such systems will continue to improve but there is continuing need to explore unique ways in which to implement such systems.

Analytic aerotriangulation has advanced very rapidly in the past decade and under ideal conditions it can now compete with geodetic surveys in the determination of survey coordinates for objects that are imaged on the photograph of interest. A certain number of control points are needed in order to perform the aerotriangulation. In most cases these objects are stationary points located at ground level. The selection of control points and the determination of these positions can take place in several ways. Basically they are determined either before the photography or after the photography. Each procedure has its advantages. In either case the flexibility of control location is limited.

The concept of a moving airborne control target offers a combination of the advantages of each control procedure mentioned above. The airborne control target can be easily seen, it can be positioned as necessary, conceptually we can have as many airborne control images as we please, they will not be destroyed or moved, and they can be commanded over inaccessible regions. What is required is that we have a sensor located at a higher altitude which will record the image of the airborne control target against the natural terrain background as well as a Distance Measurement Navigation System (DME) to continually acquire and position the airborne target

aircraft. Both sensor and navigation systems must be coupled to a precision time base.

The direct ranging or distance measurement navigation systems operate in the microwave frequency region 1,000 to 15,000 Megacycles which limits observations to line of sight. The distance measuring equipment, because of short wavelengths, can operate in either a pulse mode, transmitting a sequence of high peak power sharp rise time pulses or continuous wave mode, transmitting three or more frequencies for ambiguity resolution. Directional antennas used at ground locations yield high signal-to-noise ratios providing accuracies in the order of a few feet. Directional antennas, because of narrow beams, reduce multipath error sources. A pulse DME system is preferred for the application in this report. Large scale integrated digital circuitry produced at low cost provides an economical means of implementing selective coding features; and low cost high peak power transmitters are available for airborne transponders making the pulsed system a preferred system from economical and flexibility considerations. The high accuracy, low cost and compact size of the distance measuring system has opened up a number of applications requiring rapid deployment in areas of sparse geodetic control. A common requirement of most applications of pulsed distance measuring equipment is the accurate location of multiple ground positions in a network tied to a geodetic coordinate system.

An experimental high precision Distance Measurement System was recently installed at Rome Air Development Center.[2] The description of this distance measurement type is included as Appendix A, "Distance Measurement Equipment Navigation".

The high altitude sensor collects aerial photos which are analytically reduced based on the general bundle adjustment method. An aerial photograph is produced by a bundle of light rays that pass from object space through the camera lens to the film in the image plane. At the instant of exposure image, lens and object occupy discrete points. Knowledge of object and image positions for a finite number of rays enable the determination of the position and orientation for the aerial camera. Utilizing this camera position and orientation information, one is able to measure additional image positions and compute the location of these points in object space.

The general bundle adjustment method refers to the general case where the number of photographs and the number of rays per photo may vary as circumstance allows. The solution is a simultaneous adjustment of all rays on all photographs to produce object positions for all points of interest.

Thus the DME Navigation System provides the necessary object space control to enable the photo collection system and general bundle adjustment method to produce space positions of objects not under the control of the DME Navigation System.

Appendx B, "General Photogrammetric Bundle Adjustment Solution", describes the mathematics of the general photogrammetric bundle adjustment solution.

1.2 GENERAL SYSTEM CONCEPT AND PURPOSE OF THE INVESTIGATION

The description of the distance measuring network and remote sensing aircraft is made with reference to Figure 1 and Figure 2. Figure 1 is a typical 1:500,000 scale map showing initially installed DME ground navigation stations designated 20, 40, 70, 90 and three overlapping

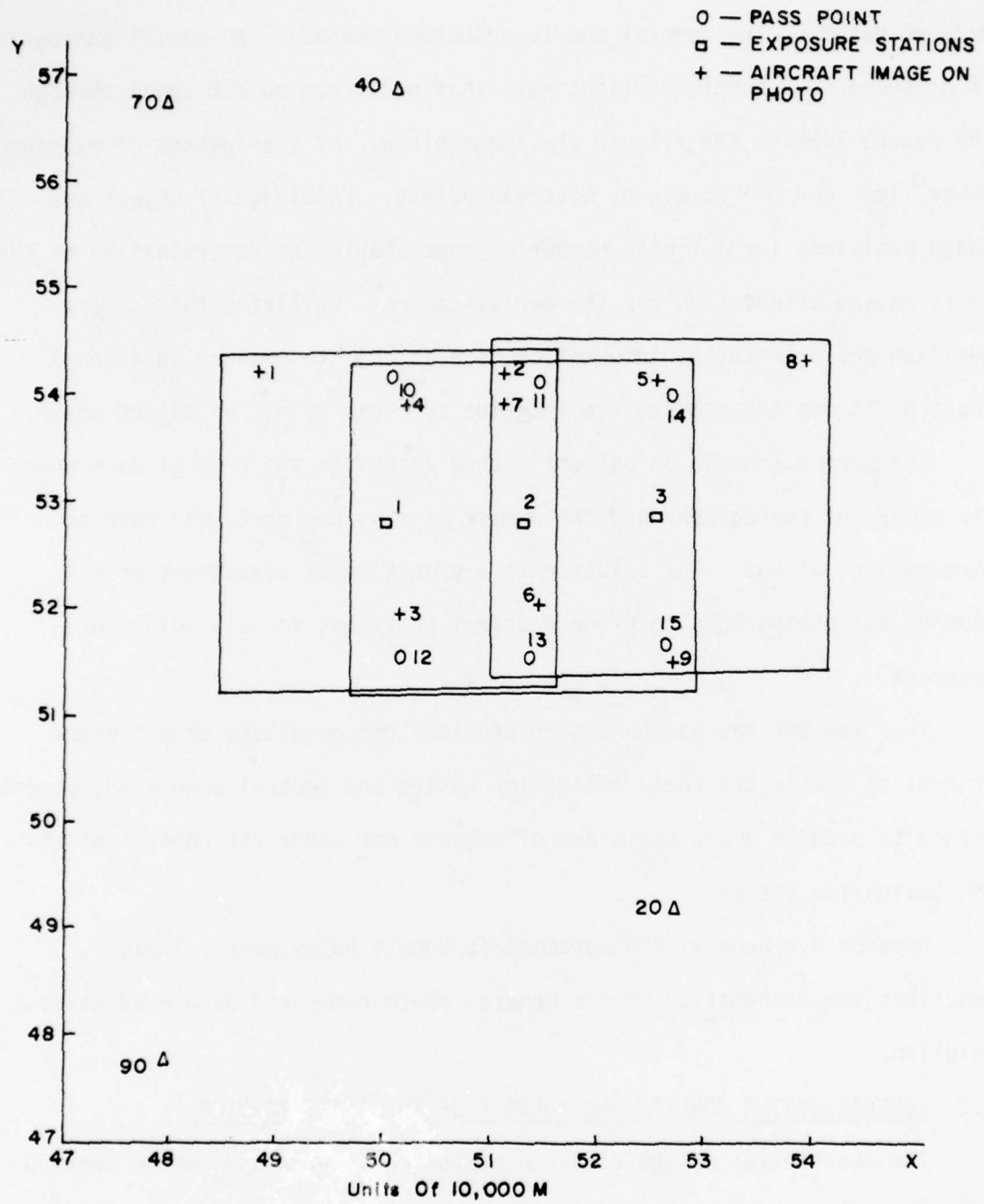

OVERLAPPING PHOTOGRAPHS ON

RADC DME NAVIGATION

SCALE 1:500,000

FIG. 1

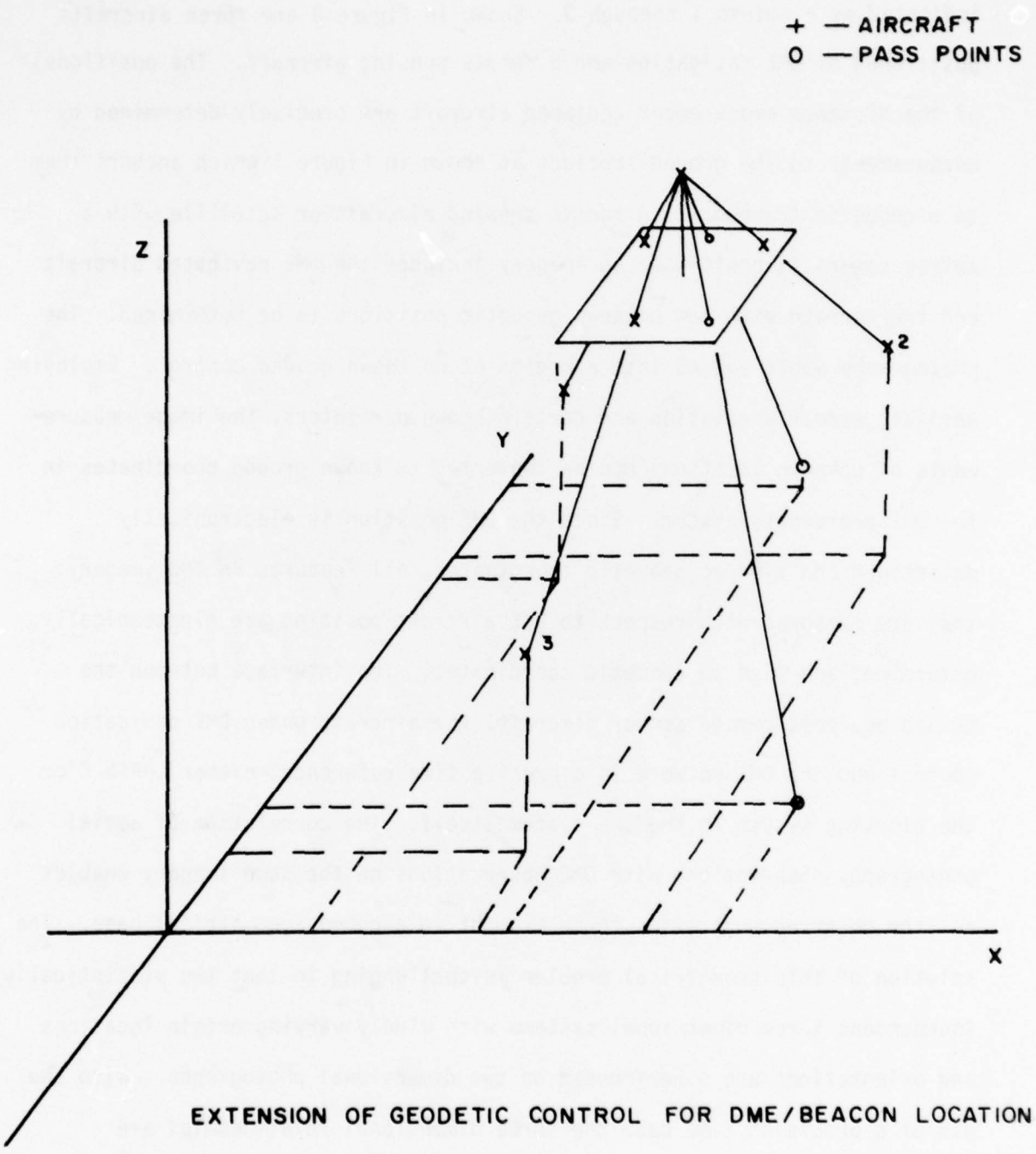

EXTENSION OF GEODETIC CONTROL FOR DME/BEACON LOCATION

FIG. 2

photo areas tied with pass points 10 through 15. Aircraft positions are indicated as + points 1 through 9. Shown in Figure 2 are three aircrafts positioned by DME navigation and a remote sensing aircraft. The positions of the distance measurement equipped aircraft are precisely determined by measurements to the ground stations as shown in Figure 1 which anchors them to a geodetic framework. A remote sensing aircraft or satellite with a metric camera is positioned so imagery includes the DME navigated aircraft and the terrain with new unknown geodetic positions to be determined. The photography would extend into a region of no known ground control. Employing analytic aerotriangulation and certain known parameters, the image measurements of unknown locations can be converted to known ground coordinates in the DME coordinate system. Since the DME position is electronically determined and tied to geodetic coordinates, all features in the imagery that are measured with respect to DME aircraft position are electronically determined and tied to geodetic coordinates. The interface between the camera equipped remote sensor aircraft, the aircraft under DME navigation control and the DME network is a precise time reference, either LORAN C or the clocking system in the DME system itself. The correlation of aerial photography observations with DME observations on the same imagery enables all the observed quantities to be brought to a common geometrical base. The solution of this geometrical problem is challenging in that two statistically independent three dimensional systems with widely varying origin locations and orientations are superimposed on two dimensional photographs. With the aid of a precision time base the three dimensional relationships are reconstructed.

The overall purpose of the study is to set up a deterministic model of the system described which will demonstrate its feasibility. Section 2 describes the investigation of combined DME and aerial photography for ground control extension. Section 3 discusses the results, and conclusions and recommendations are given in Section 4.

2.0 INVESTIGATION OF COMBINED DME AND AERIAL PHOTOGRAPHY FOR GROUND CONTROL EXTENSION

2.1 GENERAL

The object of the main experiment in this study is to test the concept of extending ground control with the aid of moving airborne targets. The experiment is comprised of four main elements. These are the control range, the narrow bandwidth real-time distance measurements from the control stations to the moving target aircraft, the wideband high resolution photography from the high altitude aircraft which images the moving target aircraft against the terrain and the analytic aerotriangulation by which the ground control is extended.

A full blown test of the procedure was not deemed practical until preliminary computations demonstrated the feasibility of the concept. In order to make the computations as realistic as possible an existing instrumentation range at Griffiss AFB, N. Y. was utilized and the experimental model was constructed to conform to the dimensions of the range. Bias errors and noise errors are measured values of the experiment.

Section 2.2 describes the instrumentation range, Section 2.3 discusses the distance measurement procedures and resulting errors, Section 2.4 covers the formation of fictitious photographs to adhere to the instrumentation range utilized in the study, and Section 2.5 provides details on the analytic aerotriangulation which was carried out to extend the ground control with moving airborne targets. The results are listed in Section 2.6.

2.2 INSTRUMENTATION RANGE AND SURVEY CONTROL

The reference range for the study was the DME Navigation Instrumentation Sites, RADC, Griffiss AFB, New York. The range has been recently surveyed

by the Geodetic Survey Squadron, F. E. Warren AFB, Wyoming.[3] The DME Navigation Range is illustrated in Figure 1. Four control stations - 20, 40, 70 and 90, were used in this study and only they are shown in Figure 1. The aircraft positions 1 through 9, as shown in Figure 1, were presumed to be located with Distance Measuring Equipment (DME). The master stations were located at stations 20, 40, 70 and 90.

Table 1 lists the local rectangular space coordinates of the above four stations together with the estimated achieved survey accuracies.

TABLE 1. SELECTED STATIONS IN THE RADC DME NAVIGATION RANGE AT GRIFFISS AFB, NEW YORK

Station	Local Rectangular Space Coordinates in Meters					
	X	$\pm\sigma_x$	Y	$\pm\sigma_y$	Z	$\pm\sigma_z$
20 (Tanner-ELS)	527028.823	±0.3	492266.378	±0.2	248.472	±0.6
40 (EP-10337)	501204.070	±0.7	568050.961	±0.3	-246.556	±0.6
70 (WP-10339)	479771.957	±0.7	566931.465	±0.3	- 72.468	±0.6
90 (RADC-ELS)	479499.707	±0.1	477793.045	±0.3	155.509	±0.4

2.3 DISTANCE MEASUREMENT AND SURVEY ERRORS

The moving airborne target procedure for control extension depends on the location of the target aircraft at the instant of the exposure of the

aerial photograph from the high altitude aircraft. All target aircraft and the photography aircraft are operating on a common time base. The error in locating the target aircraft depends upon its position in the range with respect to the tracking stations.

Assume that survey control station I is tracking aircraft J. At a given moment when the high altitude aircraft takes a photo, the distance between I and J (L_{ij}) is:

$$L_{ij} = [(X_j-X_i)^2 + (Y_j-Y_i)^2 + (Z_j-Z_i)^2]^{\frac{1}{2}} \qquad (1)$$

Thus, the coordinates of the target aircraft are:

$$X_j = [L_{ij}^2 - (Y_j-Y_i)^2 - (Z_j-Z_i)^2]^{\frac{1}{2}} + X_i$$

$$Y_j = [L_{ij}^2 - (X_j-X_i)^2 - (Z_j-Z_i)^2]^{\frac{1}{2}} + Y_i$$

$$Z_j = [L_{ij}^2 - (X_j-X_i)^2 - (Y_j-Y_i)^2]^{\frac{1}{2}} + Z_i \qquad (2)$$

Errors in X_j, Y_j and Z_j are due to the errors in the measured distance L_{ij} and the given values for the known station I (X_i, Y_i, Z_i). These errors will be designated ΔL_{ij}, ΔX_i, ΔY_i and ΔZ_i.

The error in X_j can be expressed as follows:

$$\Delta X_j = \frac{\partial X_j}{\partial L_{ij}} \Delta L_{ij} + \frac{\partial X_j}{\partial X_i} \Delta X_i + \frac{\partial X_j}{\partial Y_i} \Delta Y_i + \frac{\partial X_j}{\partial Z_i} \Delta Z_i \qquad (3)$$

Under the assumption of no correlation between the variables and the equivalence of σX_j, σX_i, σY_i and σZ_i to ΔX_j, ΔX_i, ΔY_i and ΔZ_i respectively:

$$\sigma X_j = \left[\frac{\partial X_j}{\partial L_{ij}} \sigma L_{ij}\right]^2 + \left[\frac{\partial X_j}{\partial X_i} \sigma X_i\right]^2 + \left[\frac{\partial X_j}{\partial Y_i} \sigma Y_i\right]^2 + \left[\frac{\partial X_j}{\partial Z_i} \sigma Z_i\right]^2 \quad ^{1/2} \qquad (4)$$

In a similar fashion expressions for σY_j and σZ_j can be generated. σX_i, σY_i and σZ_i values were taken from Table 1 which are the results of an actual survey. DME measurements at the RADC Navigation Range place the σL_{ij} value at 3.14 m. The DME navigation system is described in Appendix A.

Utilizing the RADC DME Navigation Range and stations 20, 40, 70 and 90 as shown in Figure 3 an error propagation study was conducted for the target aircraft located at each of the range positions (+). The value 6 m. at position $X_j = 53$, $Y_j = 53$ was the average of four X_j values computed from stations 20, 40, 70 and 90.

Figure 4 expresses the reliability of the values given in Figure 3. Similarly, Figures 5 and 6 express the error propagation in Y_j and Figures 7 and 8 apply to the Z_j coordinate of the target aircraft.

The resultant errors are displayed in Figure 9 along with standard deviation values.

where:

$$\text{Resultant} = [X_j^2 + Y_j^2 + Z_j^2]^{1/2} \qquad (5)$$

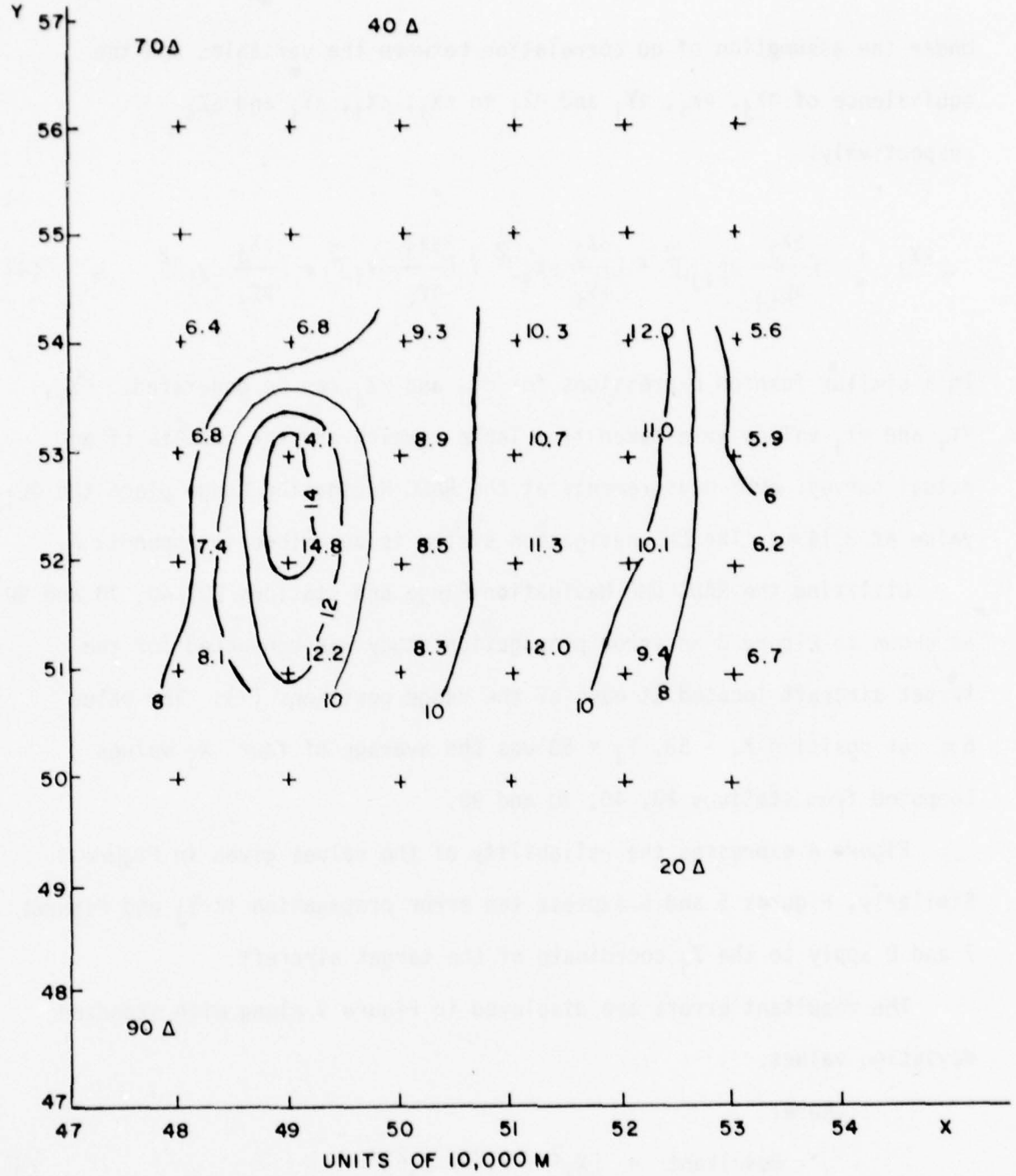

AVERAGE ERROR IN X (METERS)

RADC DME NAVIGATION RANGE

SCALE 1:500,000

FIG.3

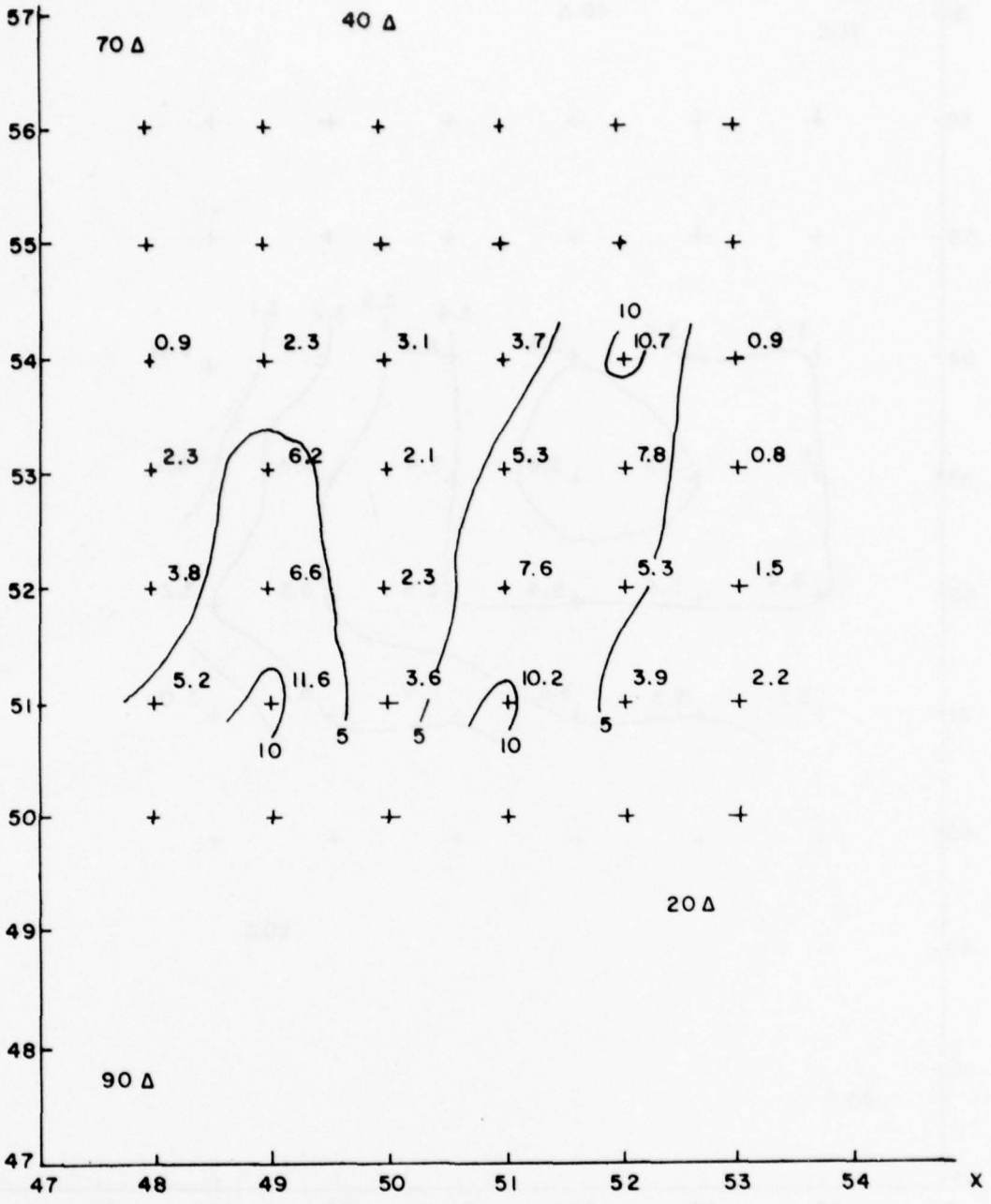

UNITS OF 10,000 M

STANDARD DEVIATION IN X BASED ON FOUR VALUES (METERS)

RADC DME NAVIGATION RANGE

SCALE 1:500,000

FIG. 4

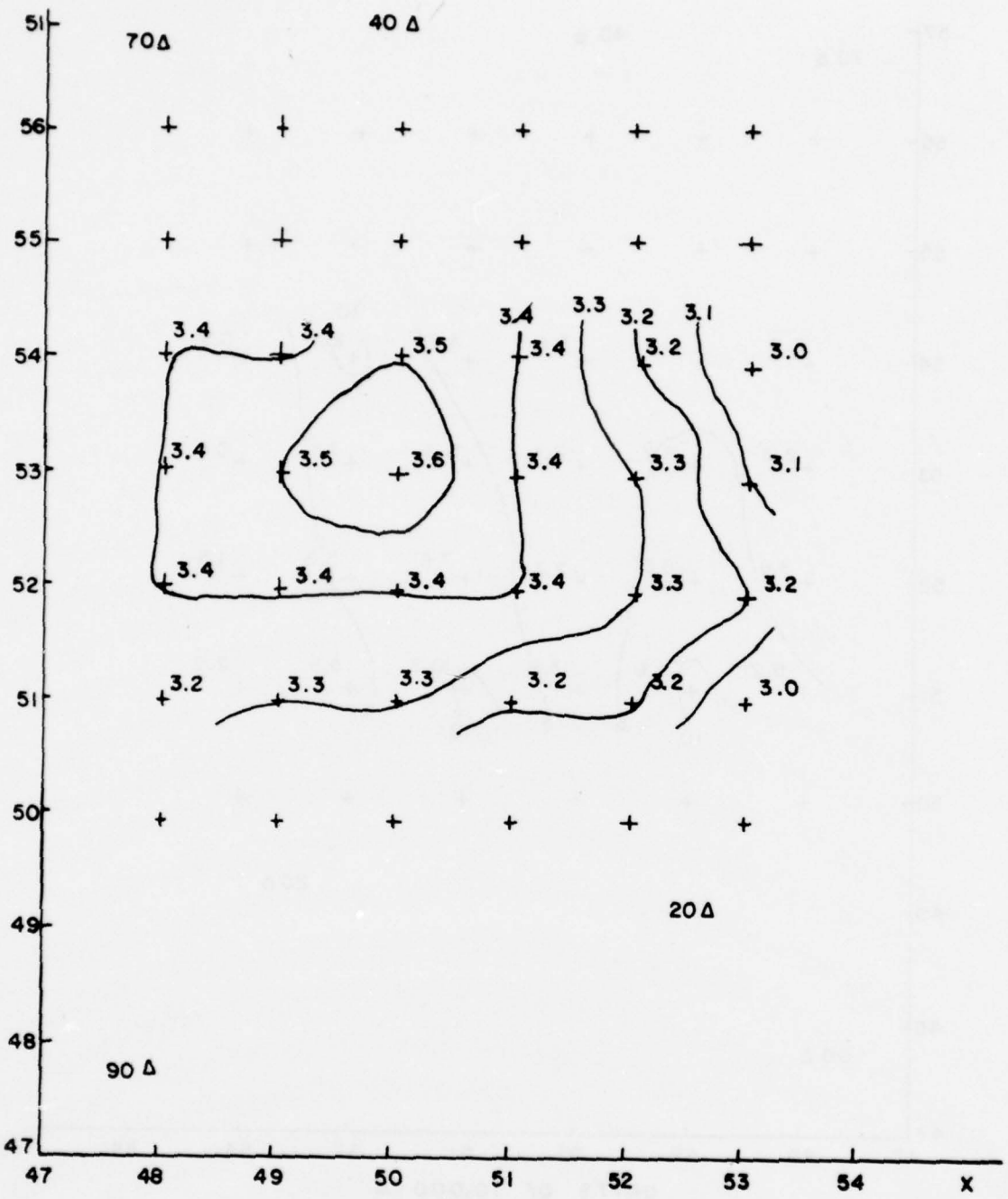

UNITS OF 10,000 M

AVERAGE ERROR IN Y (METERS)

RADC DME NAVIGATION RANGE

SCALE 1:500,000

FIG. 5

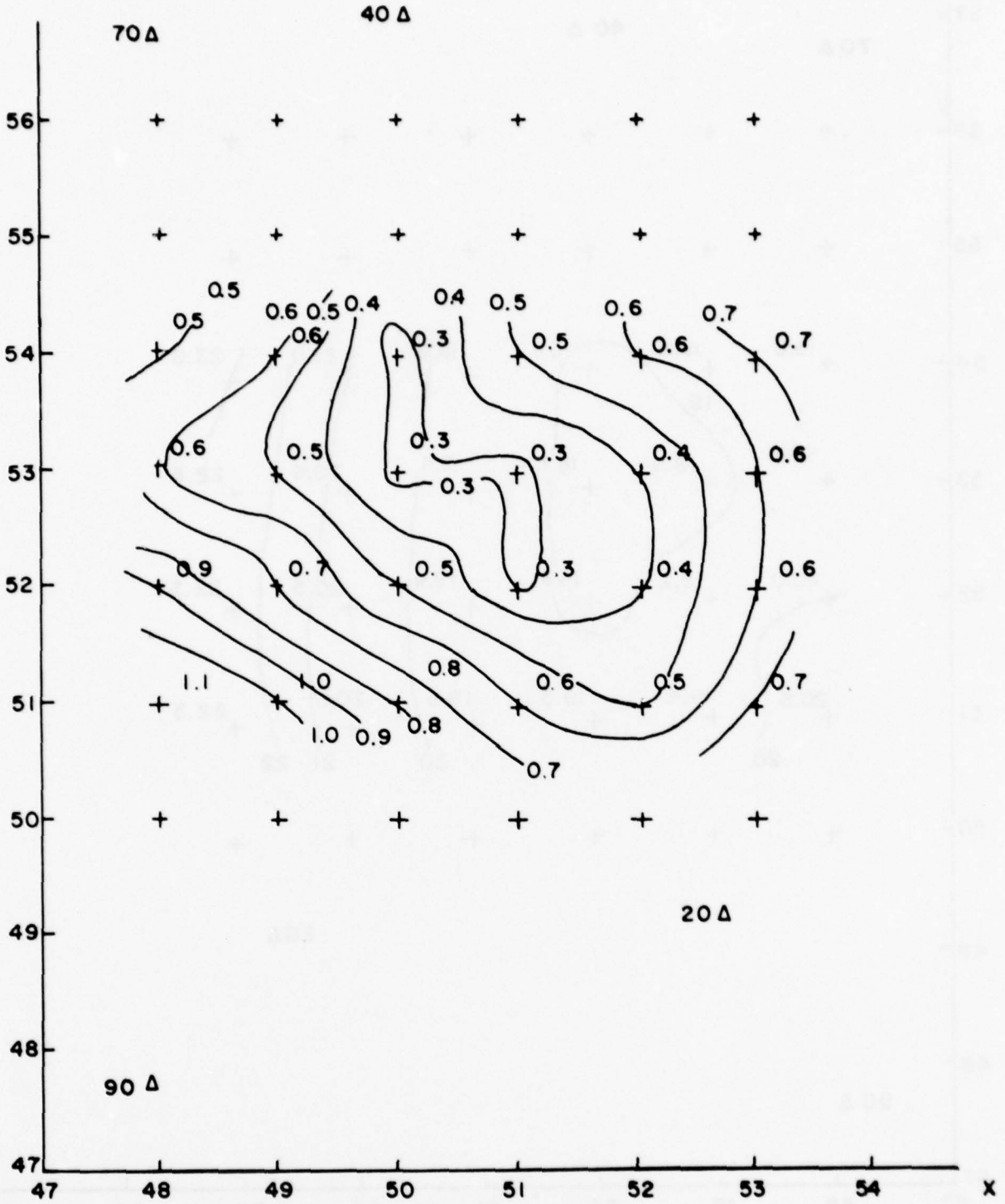

UNITS OF 10,000 M

STANDARD DEVIATION IN Y (METERS)

RADC DME NAVIGATION RANGE

SCALE 1:500,000

FIG. 6

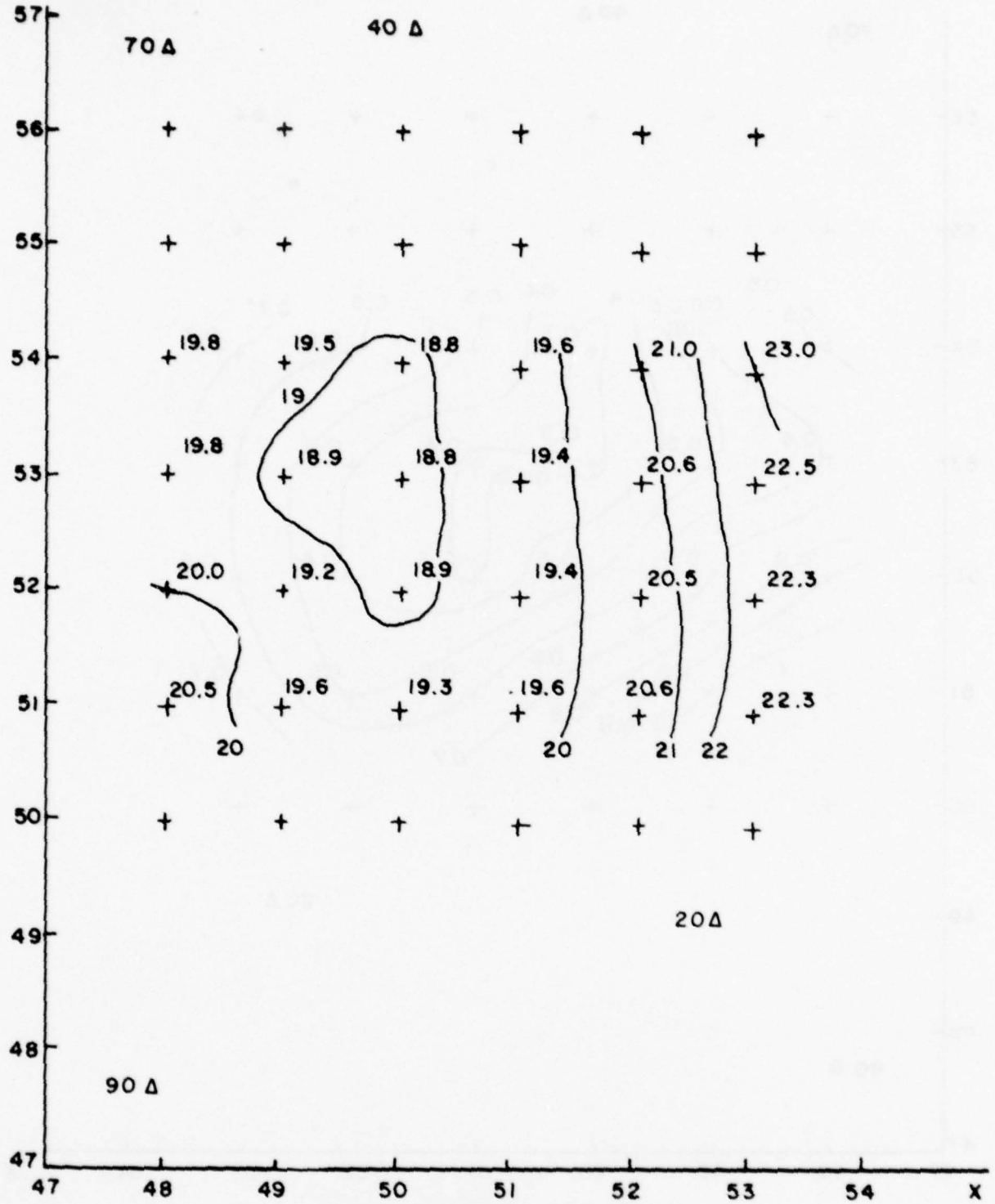

UNITS OF 10,000 M

AVERAGE ERROR IN Z (METERS)

RADC DME NAVIGATION

SCALE 1:500,000

FIG. 7

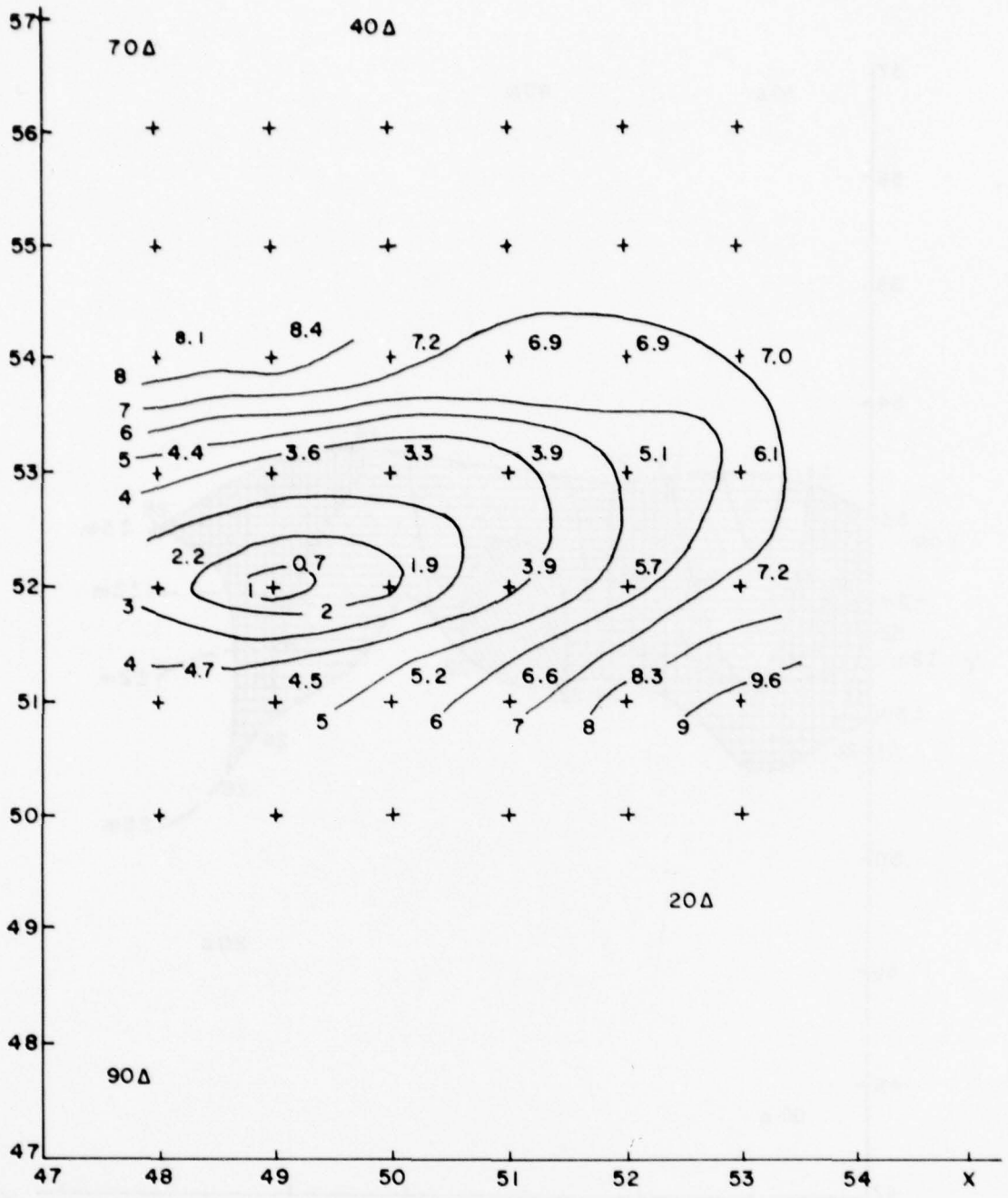

UNITS OF 10,000 M

STANDARD DEVIATION IN Z (METERS)

RADC DME NAVIGATION

SCALE 1:500,000

FIG. 8

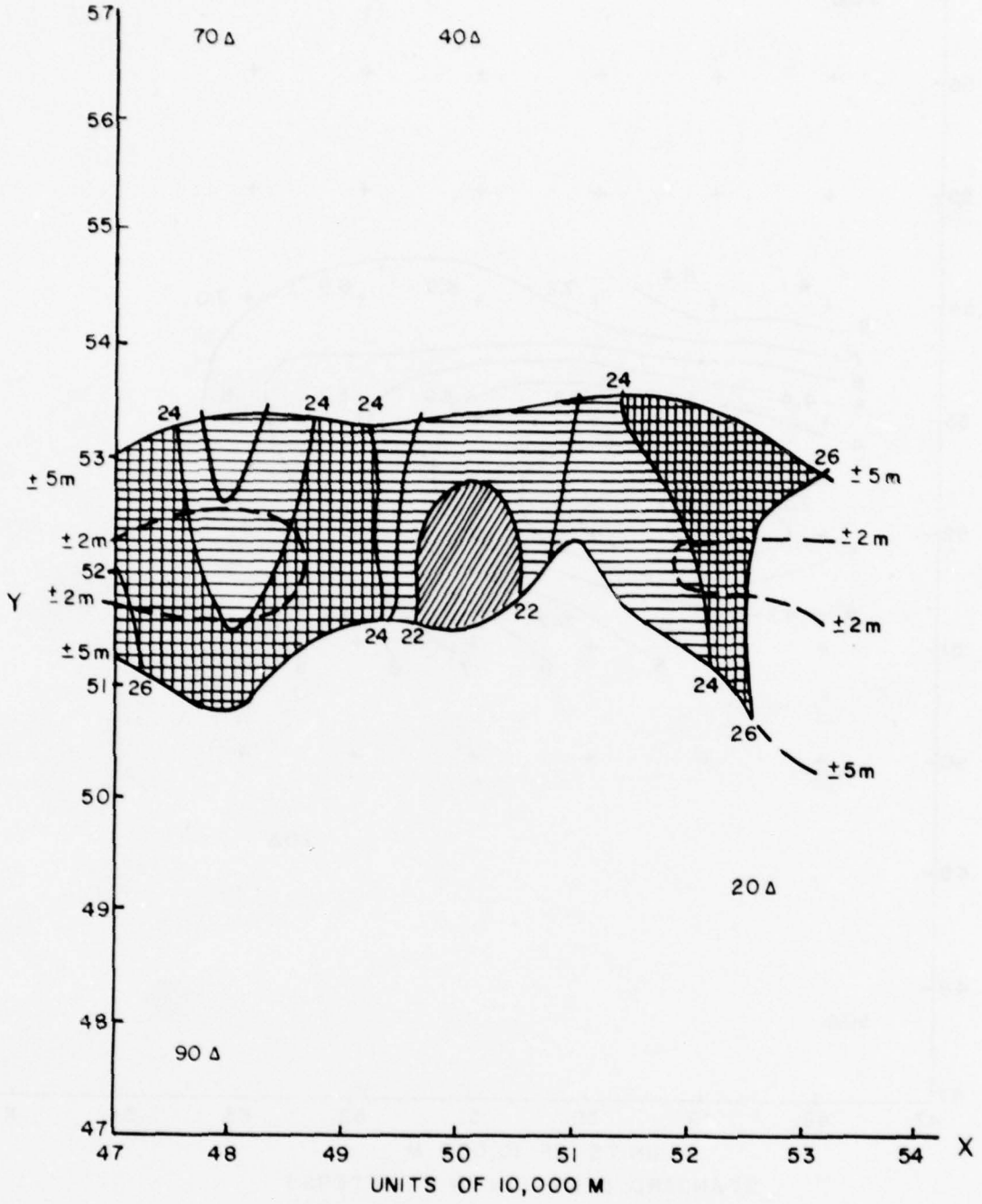

RADC DME NAVIGATION

SCALE 1:500,000

RESULTANT ERRORS IN METERS WITH S.D.

R=20-22 R=22-24 R=24-26

FIG. 9

It should be noted that 70 to 80 percent of the error values in Figure 9 are due to the error propagation in Z. The planimetric errors over this area of the range would average about 10 meters.

2.4 HIGH ALTITUDE PHOTOGRAPHY

The general concept of the use of high altitude photography of moving airborne targets against the natural terrain background is shown in Figure 2. The high altitude aircraft exposes a photo and images two types of points. The first is the moving airborne targets for which X, Y, and Z are known. The second is pass points whose X, Y, and Z coordinates must be computed.

In this study three fictitious high altitude photographs were created. Figure 1 illustrates the position and extent of coverage of these photos within the RADC DME Navigation Range.

Tables 2, 3 and 4 summarize the parameters of the three fictitious high altitude photographs.

2.5 ANALYTIC AEROTRIANGULATION COMPUTATIONS

Utilizing the RADC DME Navigation Range and a standard bundle adjustment solution, a fictitious flight line of three consecutive aerial photographs was triangulated for the solution of six unknown ground points and the three exposure stations. Figure 1 shows the location of the photos within the range. Recall that points 1 through 9 are aircraft which are located by DME and appear on the photos as targets. Points 10 through 15 are selected pass point images whose range coordinates will be determined as a result of the analytic aerotriangulation.

The input to the solution includes the DME determined aircraft coordinates and the photo coordinates of the aircraft and selected

TABLE 2. FICTITIOUS HIGH ALTITUDE PHOTO NO. 1

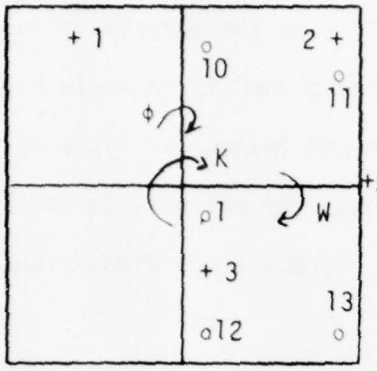

X_1^C=500,500 m. x_{p1}=0 mm.

Y_1^C=527,400 m. y_{p1}=0 mm.

Z_1^C=20,000 m. f=152.4 mm.

K=0°30' + - Moving Airborne Targets

φ=1°30' 0 - Pass Points

W=0°30' f - Focal Length

x_1	-78.185*	x_2	74.977	x_3	3.522	x_{10}	+3.000
y_1	98.988	y_2	100.790	y_3	-53.749	y_{10}	+100.000
X_1	495,000.000**	X_2	505,000.000	X_3	500,500.000	X_{10}	500,256.576
Y_1	534,000.000	Y_2	534,000.000	Y_3	524,000.000	Y_{10}	540,643.380
Z_1	10100.000	Z_2	10150.000	Z_3	10,075.000	Z_{10}	200.000

x_{11}	104.000	x_{12}	2.000	x_{13}	98.000
y_{11}	105.000	y_{12}	-90.000	y_{13}	-95.000
X_{11}	513,322.474	X_{12}	500,344.655	X_{13}	512,637.071
Y_{11}	541,283.620	Y_{12}	515,972.132	Y_{13}	515,521.093
Z_{11}	50.000	Z_{12}	250.000	Z_{13}	60.000

* - Photo Coordinate in mm.

** - Range Coordinate in m.

TABLE 3. FICTITIOUS HIGH ALTITUDE PHOTO NO. 2

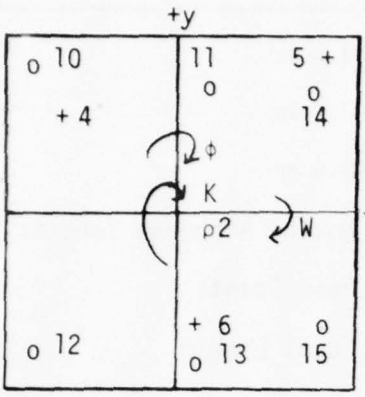

X_2^C=512,000 m. x_{p2}=0.0 mm.

Y_2^C=528,500 m. y_{p2}=0.0 mm.

Z_2^C=20,000 m. f=152.4 mm.

K=0°30' + - Moving Airborne Targets

φ=1° 0 - Pass Points

W=0°45' f - Focal Length

x_4	-78.189*	x_5	96.194	x_6	9.572
y_4	87.734	y_5	100.603	y_6	-86.401
X_4	506,500.000**	X_5	518,000.000	X_6	512,500.000
Y_4	534,500.000	Y_5	535,200.000	Y_6	523,000.000
Z_4	10,100.000	Z_5	10,310.000	Z_6	10,175.000
x_{10}	-84.480	x_{11}	13.415	x_{12}	-87.083
y_{10}	89.674	y_{11}	93.919	y_{12}	-97.762
X_{10}	500,256.576	X_{11}	513,322.474	X_{12}	500,344.655
Y_{10}	540,643.380	Y_{11}	541,283.620	Y_{12}	515,972.132
Z_{10}	200.000	Z_{11}	50.000	Z_{12}	250.000
x_{13}	6.644	x_{14}	99.000	x_{15}	90.000
y_{13}	-101.193	y_{14}	93.000	y_{15}	-85.000
X_{13}	512,637.071	X_{14}	524,372.360	X_{15}	523,302.770
Y_{13}	515.521.093	Y_{14}	540,918.912	Y_{15}	517,951.376
Z_{13}	60.000	Z_{14}	400.000	Z_{15}	300.000

* - Photo Coordinate in mm.
** - Range Coordinate in m.

TABLE 4. FICTITIOUS HIGH ALTITUDE PHOTO NO. 3

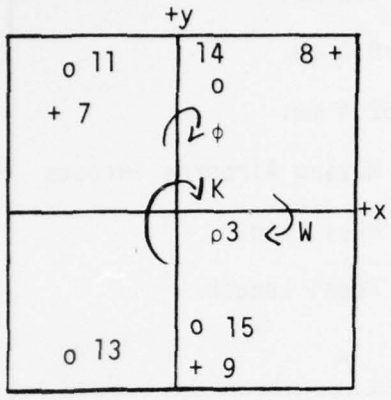

X_3^C=523,000 m.	x_{p3}=0.0 mm.
Y_3^C=529,000 m.	y_{p3}=0.0 mm.
Z_3^C=20,100 m.	f=152.4 mm.
K=1°	+ - Moving Airborne Targets
φ=2°	0 - Pass Points
W=1°	f - Focal Length

x_7	-85.000	x_8	+92.000	x_9	+2.000	x_{11}	-64.811
y_7	+88.000	y_8	+90.000	y_9	-101.000	y_{11}	89.474
X_7	516,787,773	X_8	528,472.625	X_9	522,899,415	X_{11}	513,322.474
Y_7	535,029.936	Y_8	535,067.862	Y_9	522,657.776	Y_{11}	541,283.620
Z_7	10,100	Z_8	10,200	Z_9	10,150	Z_{11}	50.000

x_{13}	-74.912	x_{14}	17.416	x_{15}	6.131
y_{13}	-103.276	y_{14}	88.587	y_{15}	-88.786
X_{13}	512,637.071	X_{14}	524,372.360	X_{15}	523,302.770
Y_{13}	515,521.093	Y_{14}	540,918.912	Y_{15}	517,951.376
Z_{13}	60.000	Z_{14}	400.000	Z_{15}	300.000

* - Photo Coordinate in mm.
** - Range Coordinate in m.

pass points. Since these are measured quantities a weight is assigned to each of the values. Approximations are assigned to the unknown quantities, namely, the outer orientation values and the unknown range coordinates for the pass points. Weights are used as constraints in the solution and accordingly the approximate values are given a weight of zero so that they may have complete freedom in the solution and obtain their most probable values.

Twelve aerotriangulation solutions were computed. The following four had particular significance.

1) Solution 1 - The purpose of this solution was to demonstrate that the deterministic aerotriangulation model and computational procedure were correct. All input control and coordinate information are correct and the solution converges to the correct values for the outer orientation parameters and the range coordinates for the pass points.

2) Solution 2 - In this solution the range coordinates of the target aircraft were perturbed according to the error propagation resulting from DME and ground station survey errors. The appropriate X, Y and Z errors were selected from Figures 3, 5 and 7. Signs for these error values were selected from a table of random numbers. A weight of unity was used for the above coordinates. The photo coordinates were given the weight of 2500 in this solution. This assumes a 20 micrometer standard deviation in each photo coordinate.

3) Solution 3 - In this solution the range coordinates of the target aircraft were perturbed in the same manner as in solution 2. However, in this solution the weights used for the above coordinates reflect the error

introduced into the coordinate. The weight of the X coordinate of target aircraft 1 is 0.02 since,

$$W_1 = \frac{1}{\sigma X1^2} = \frac{1}{7^2} = .02$$

thus reflecting the 7 meter error introduced into X_1.

The photo coordinates were given the weight of 2500 in this solution. This assumes a 20 micrometer standard deviation in each photo coordinate.

4) Solution 4 - This solution was similar to 3 except that the photo coordinates in this case were weighted 500 rather than 2500. Thus, it was assumed that each photo coordinate may have a standard deviation of 45 micrometers.

2.6 RESULTS OF ANALYTIC AEROTRIANGULATION

The purpose of this study was to demonstrate how moving airborne targets could be utilized to extend ground control. The results are presented in the form of a number of figures showing the area of the range that control was being extended into and the actual errors that resulted from the aerotriangulation as previously described. Error is defined as the absolute value in meters between the known coordinate from the deterministic model and the final coordinate values given by the analytic aerotriangulation solution.

The results of solution 2 are illustrated in Figure 10. The values in the parenthesis are the absolute resultant errors that apply to the nearest pass point or exposure station. Resultant is defined in equation (5). $\overline{X}_R$ equals the average resultant error to the nearest meter for the

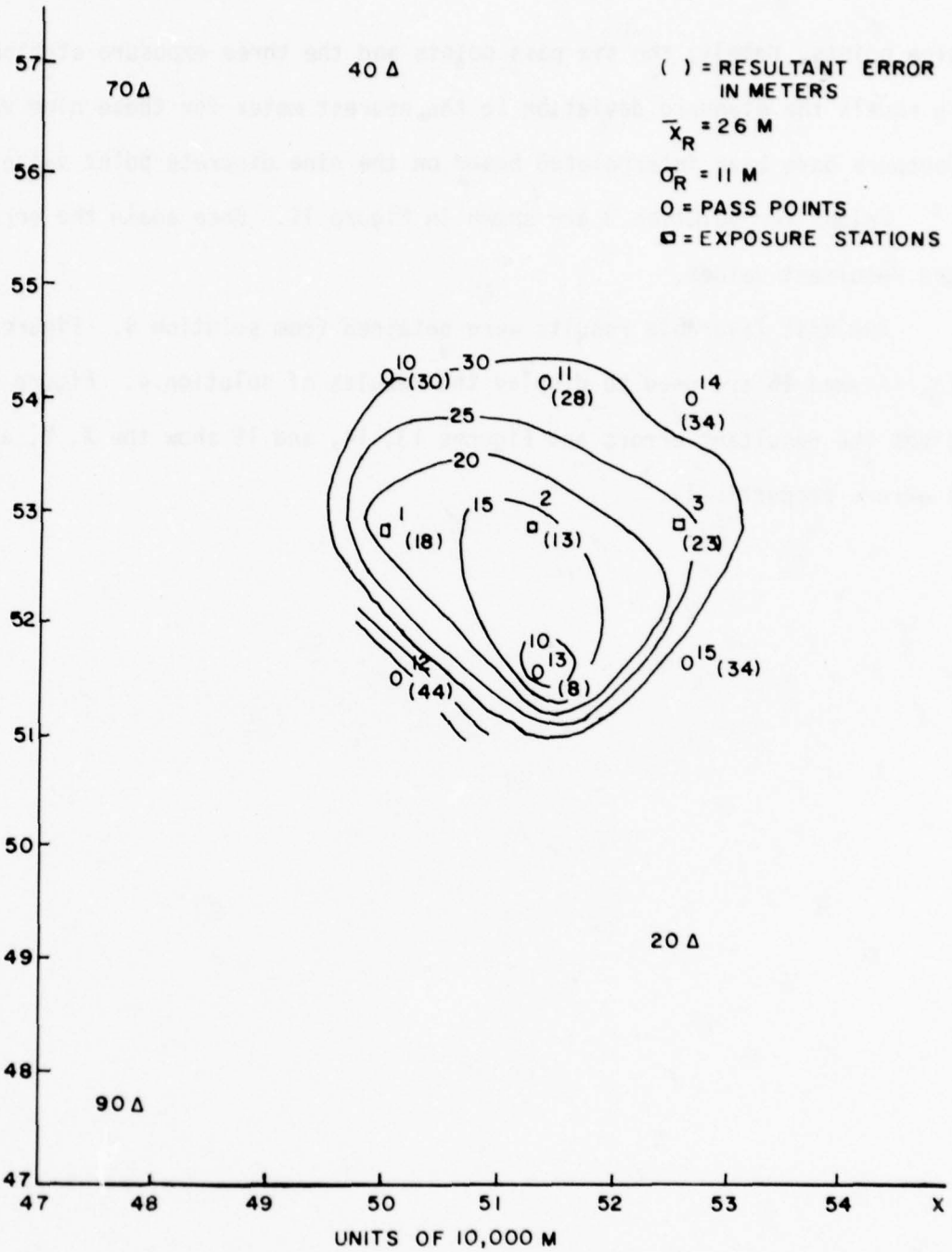

AEROTRIANGULATION RESULTS UTILIZING ERROR PROPAGATED CONTROL

ALL CONTROL COORDINATES WEIGHTED UNITY

SCALE 1:500,000

FIG. 10

nine points, namely; the six pass points and the three exposure stations. σ_R equals the standard deviation to the nearest meter for these nine values. Contours have been interpolated based on the nine discrete point values.

Values for solution 3 are shown in Figure 11. Once again the errors are resultant values.

The most favorable results were obtained from solution 4. Figures 12, 13, 14, and 15 are used to display the results of solution 4. Figure 12 gives the resultant errors and Figures 13, 14, and 15 show the X, Y, and Z errors respectively.

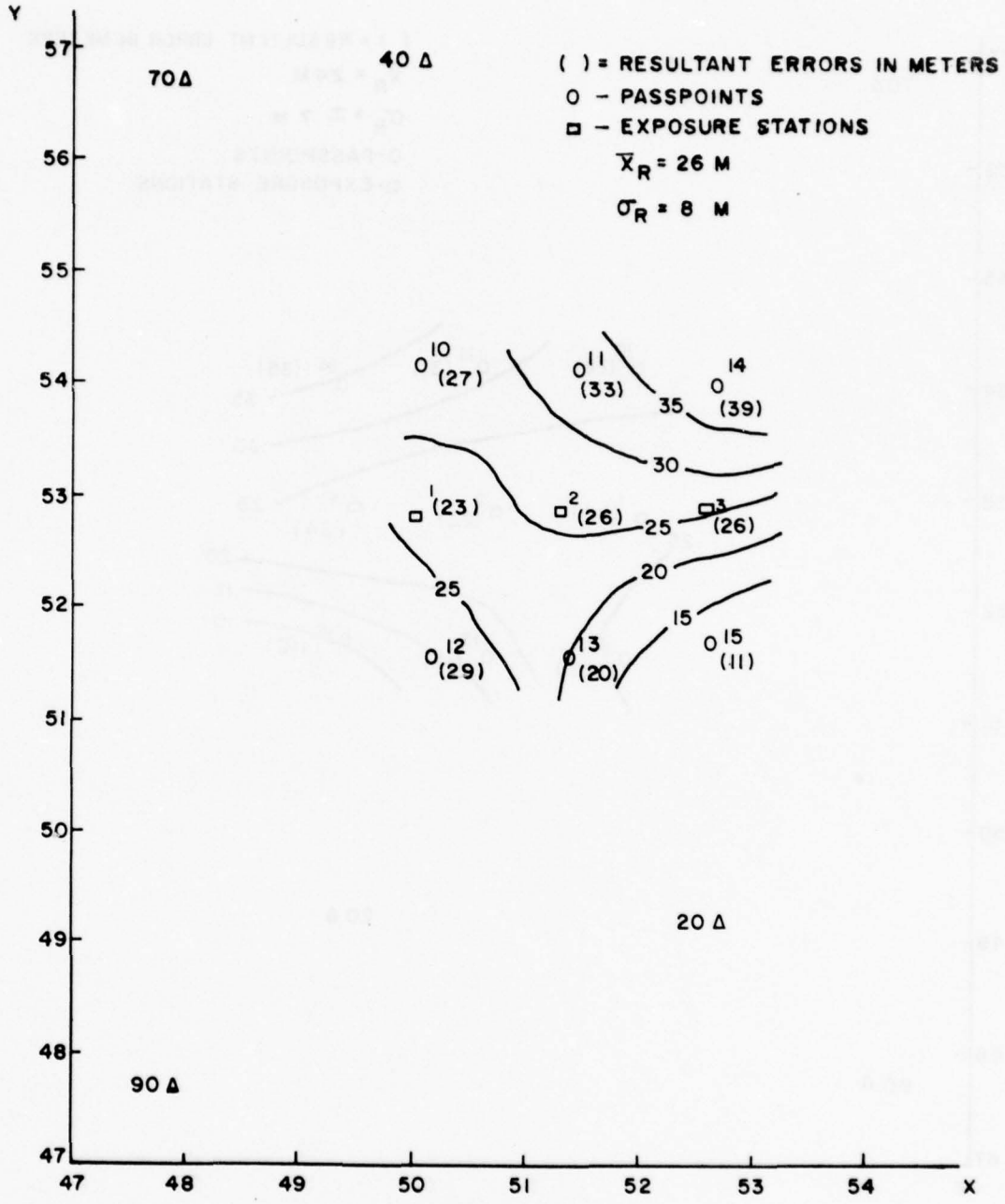

UNITS OF 10,000 M

AEROTRIANGULATION RESULTS UTILIZING ERROR PROPAGATED CONTROL

WEIGHT OF CONTROL COORDINATES EQUALS $1:(\text{ERROR})^2$

WEIGHT OF PHOTO COORDINATES EQUALS 2500

SCALE 1:500,000

FIG. 11

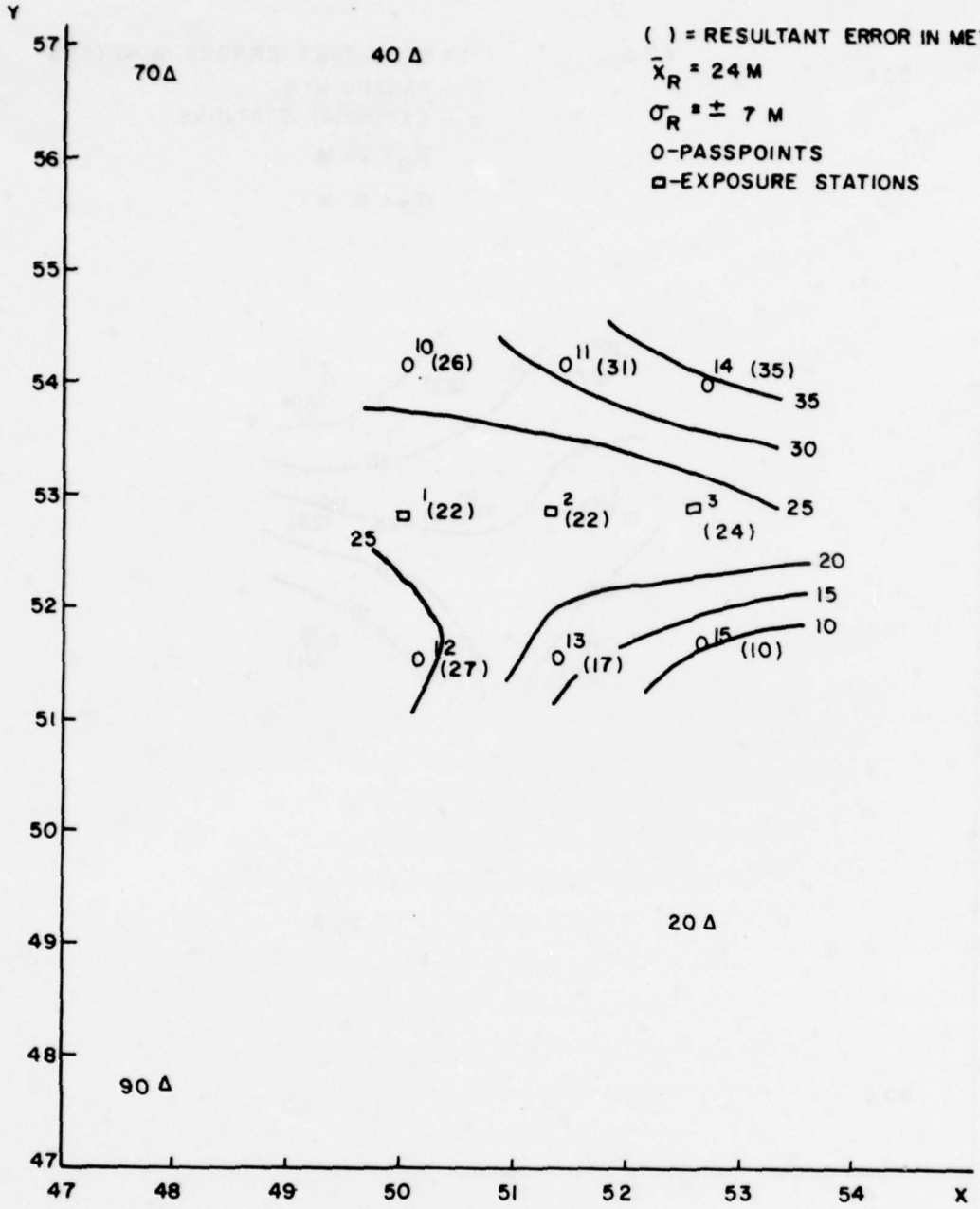

UNITS OF 10,000 M

AEROTRIANGULATION RESULTS UTILIZING ERROR PROPAGATED CONTROL

WEIGHT OF CONTROL COORDINATES EQUALS $1:(\text{ERROR})^2$

WEIGHT OF PHOTO COORDINATES EQUALS 500

SCALE 1:500,000

FIG. 12

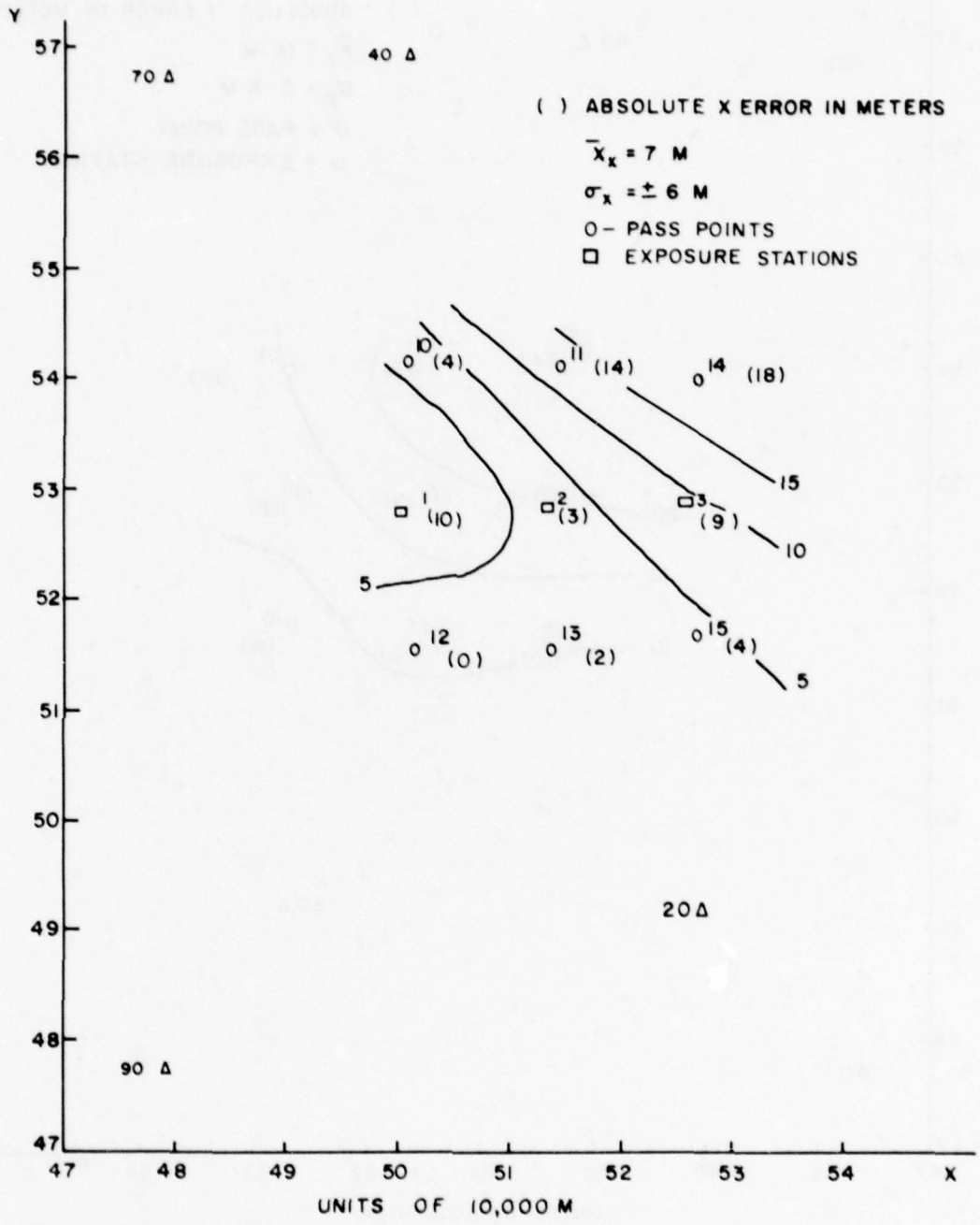

AEROTRIANGLATION RESULTS UTILIZING ERROR PROPAGATED CONTROL

WEIGHT OF CONTROL COORDINATES EQUALS $1:(\text{ERROR})^2$
WEIGHT OF PHOTO COORDINATES EQUALS 500

SCALE 1:500,000

FIG. 13

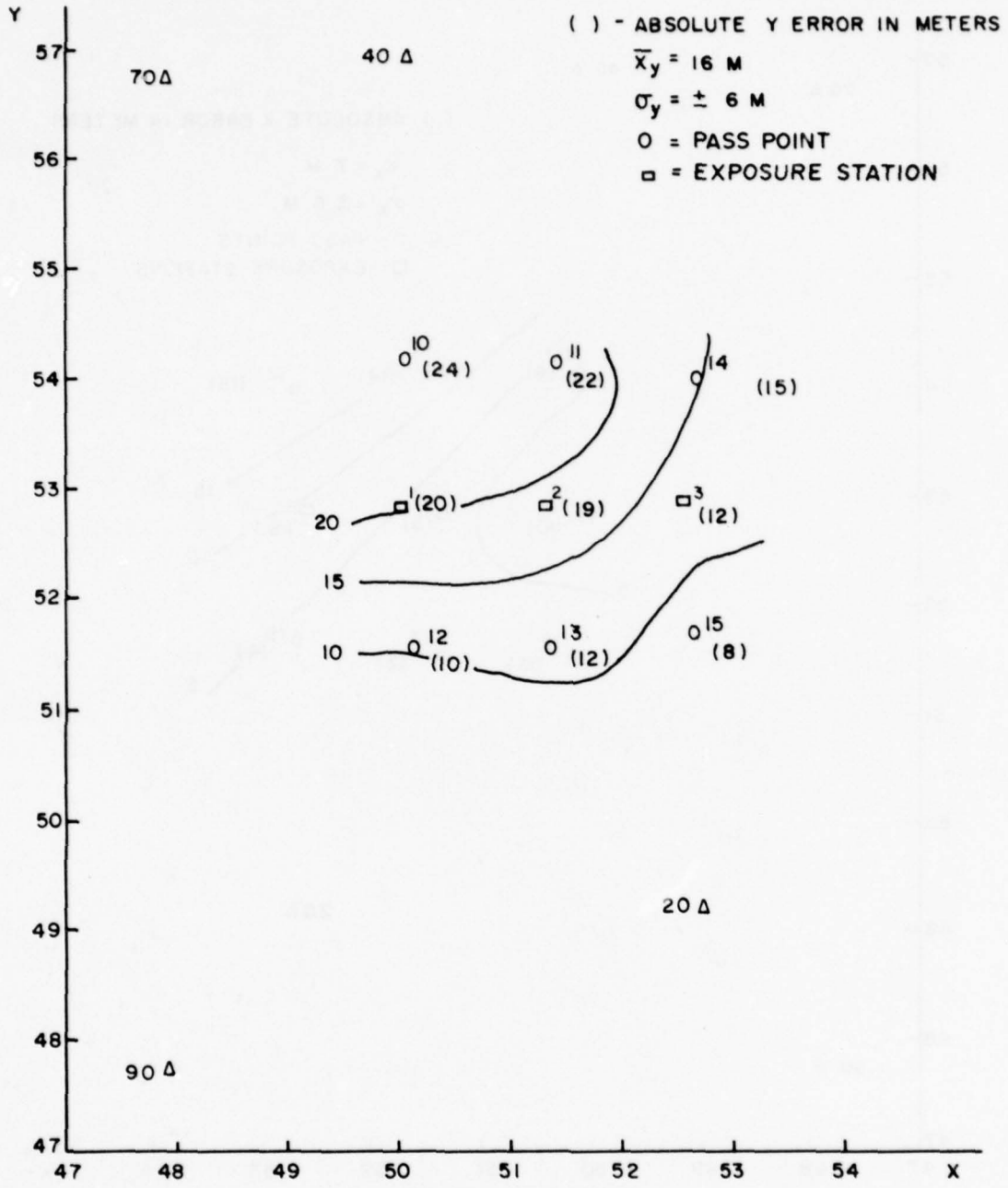

UNITS OF 10,000 M

AEROTRIANGULATION RESULTS UTILIZING ERROR PROPAGATED CONTROL

WEIGHT OF CONTROL COORDINATES EQUALS $1:(\text{ERROR})^2$

WEIGHT OF PHOTO COORDINATES EQUALS 500

SCALE 1:500,000

FIG. 14

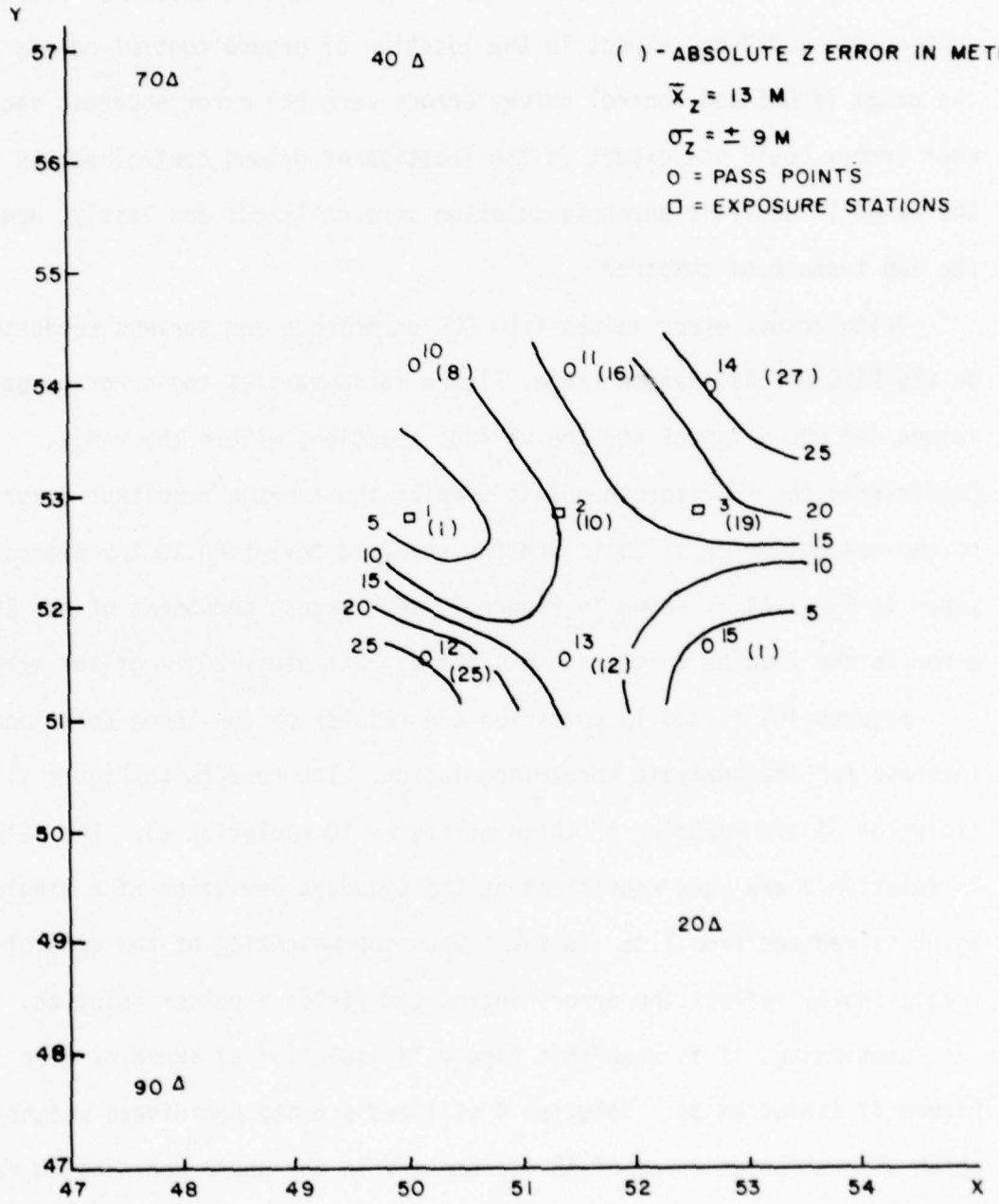

UNITS OF 10,000 M

AEROTRIANGULATION RESULTS UTILIZING ERROR PROPAGATED CONTROL

WEIGHT OF CONTROL COORDINATES EQUALS 1: (ERROR)^2

WEIGHT OF PHOTO COORDINATES EQUALS 500

SCALE 1:500,000

FIG. 15

3.0 DISCUSSION OF RESULTS

The results will be discussed in terms of three questions. First, what errors could one expect in the location of ground control points in the range if DME and control survey errors were the error sources; second, what errors could one expect in the location of ground control points in the range if analytic aerotriangulation were utilized; and lastly, how do the two techniques compare?

Using actual error values from DME experience and surveys conducted on the RADC DME Navigation Range, Figure 16 summarizes the error propagation values one would expect for the various locations within the range. Considering the 49 discrete points sampled the average resultant error to the nearest meter is 25 m. and the standard deviation to the nearest meter is 2 m. As is shown in Figure 7, the largest component of the 25 m. error is the Z value which accounts for approximately 20 m. of the error.

Figures 10, 11 and 12 summarize the results of the three solutions of interest for the analytic aerotriangulation. The results in Figure 11 (solution 3) are superior to those of Figure 10 (solution 2). The values in solution 3 are more consistent as the standard deviation of a single point is reduced from 11 m. to 8 m. Thus the weighting of the control to realistically reflect the errors introduced yields a better solution.

Continuing, it is seen that Figure 12 (solution 4) improves over Figure 11 (solution 3). Solution 4 utilized a photo coordinate weighting which allows for an error of 45 micrometers in the photo coordinates rather than the 20 micrometers that was allowed in solution 3. In effect the photo coordinates in 4 were allowed more flexibility in seeking the best-fit solution. Under the dynamic conditions for the moving airborne

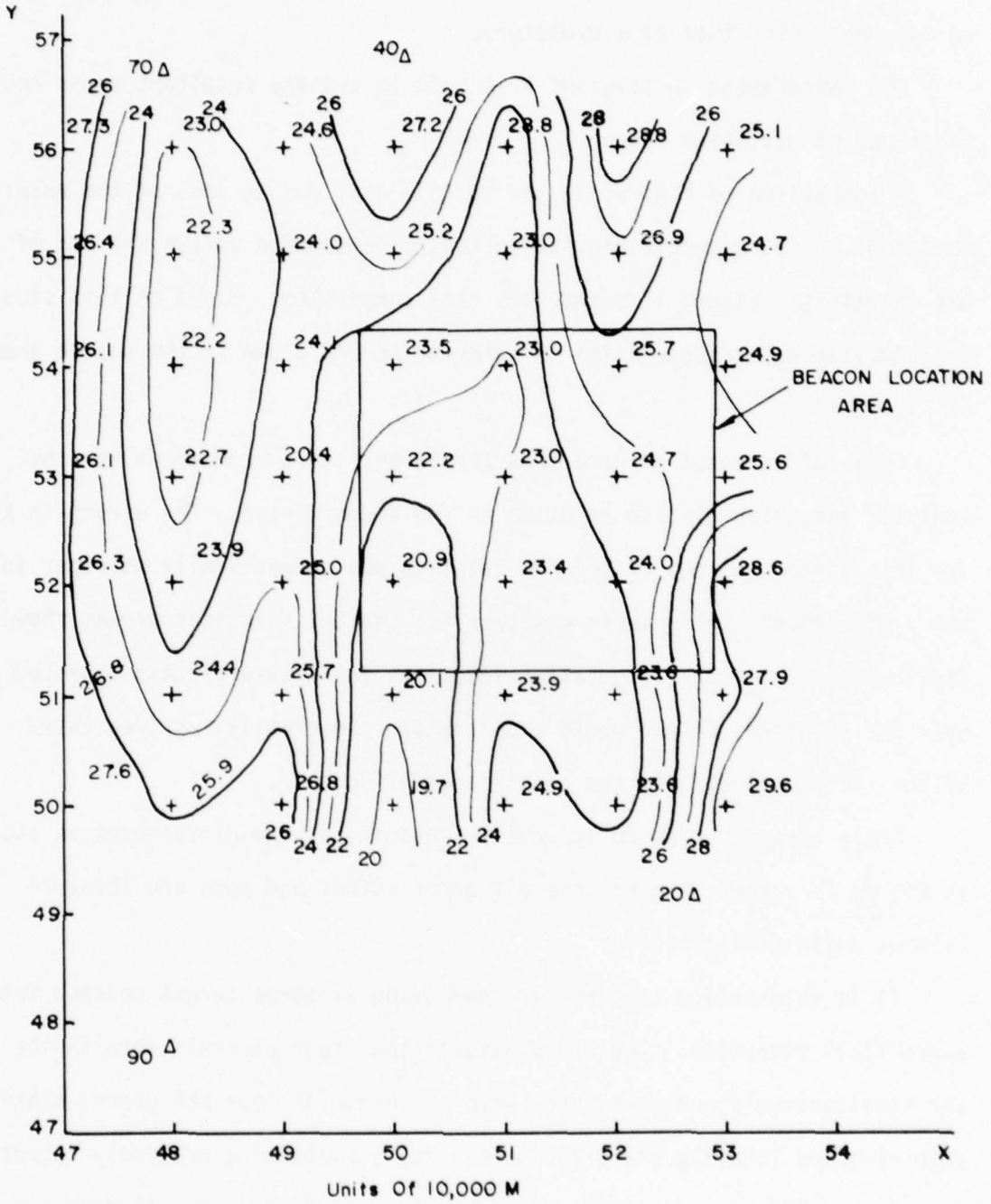

PROPAGATION OF DME AND SURVEY ERRORS

VALUES SHOWN ARE THE AVERAGE RESULTANT ERRORS IN METERS

FROM STATIONS 20, 40, 70 & 90

SCALE 1:500,000

FIG. 16

targets, the 45 micrometer flexibility in photo coordinates may very well be more realistic than 20 micrometers.

The improvement in solution 4 is both in average resultant error and the standard deviation value.

A comparison of Figures 12 and 16 will give one an idea of the relative merits of analytic aerotriangulation control extension versus the use of the DME solutions. Figure 17 summarizes this comparison. Based on this study the analytic aerotriangulation is superior to DME alone in the shaded areas of Figure 17.

It is of interest to note that the largest error component for the analytic aerotriangulation solution is the Y coordinate. The errors in X are less since the control for the solution was geometrically stronger in the X direction. The reverse was true for the DME solutions as was shown previously. The aerotriangulation solutions for Z were greatly improved over DME solutions as one would expect under the greatly improved base/height ratios existing in the aerotriangulation case.

There appears to be no systematic reasons for the differences as shown in Figure 17. Keep in mind that all error values and sums are absolute without defined direction.

It is interesting to consider the moving airborne target concept from a practical viewpoint. The study assumes that four aircraft were in the air simultaneously and that there were a minimum of four DME ground stations acquiring and locating the airborne control targets on a precisely coordinated time base. This is admittedly an elaborate system, however, it does result in the location of ground stations without occupying the stations or, in fact, being able to directly view them. DME solutions alone would require

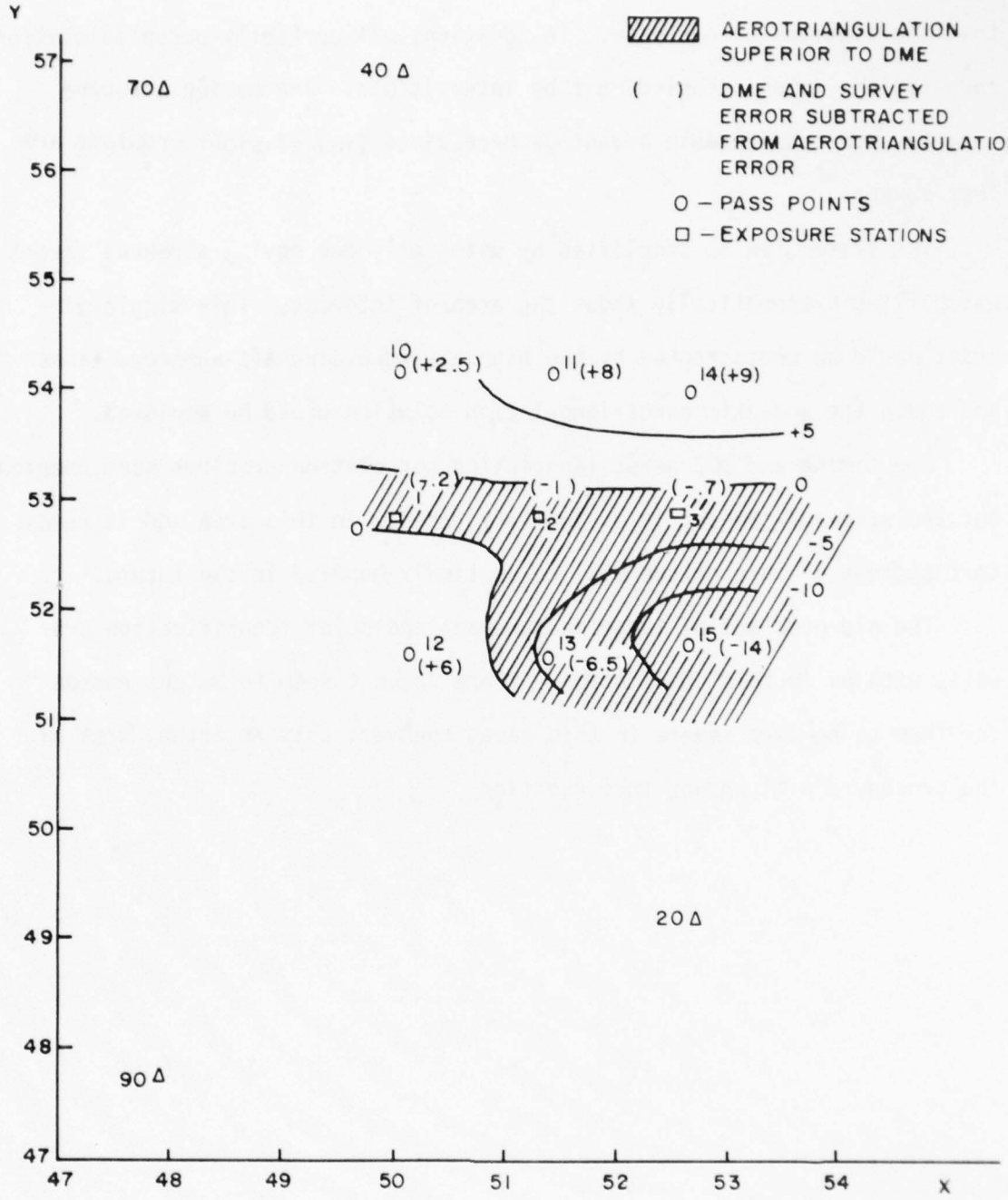

AEROTRIANGULATION ERRORS LESS DME AND SURVEY ERRORS

SCALE 1:500,000

FIG. 17

that the stations be occupied. In addition, all currently occupied stations and stations to be occupied must be intervisible. The moving airborne targets have considerable advantage here since line-of-sight problems are less severe.

The system can be simplified by using only one moving airborne target which flies systematically about the area of interest. This single aircraft would be photographed by the high altitude aircraft numerous times and again the analytic aerotriangulation solution would be employed.

The timing and DME aerotriangulation correlation problems seem complex but the state-of-the-art is moving very rapidly in this area and it seems that systems of this nature will be routinely handled in the future.

The old problems of image measurement and point identification are still with us in this application. There doesn't seem to be any reason for them to be more severe in this case, however, only an actual test of the procedure will answer this question.

4.0 CONCLUSIONS AND RECOMMENDATIONS

The following conclusions have been drawn from the study.

1) Narrowband distance measurements have been successfully combined with wideband photography for the extension of range control. There is an indication that the concept may be as good as standard ground techniques for ground control extension.

2) The moving airborne target technique is very flexible and photo flight lines can be run which, due to superior geometry and redundant sampling, provide small errors in X, Y and Z coordinates. The flight line orientation in the subject study favored the X coordinate. Command of the aircraft flight path to selected areas can minimize errors. The desired geographical flight areas can be determined prior to aircraft flight.

3) The procedures described represent an order of magnitude decrease in the time required to perform ground surveys to DME navigation system requirements.

4) The feasibility of the procedure will improve as each of the system components approaches a real time capability. This includes real-time data reduction by the DME, together with the use of high resolution charge coupled device cameras programmed for real time solutions.

The following recommendations are made:

1) Additional effort needs to be expended to determine the most efficient use of the moving airborne target concept.

2) This technique applies a combination of DME and photo sensing instruments. Similar concepts using a combination of other sensors should be explored. In this way each sensor can contribute its outstanding characteristic to the total mission.

REFERENCES

1. DiCarlo, C. and Eakin, G., Mapping and Survey System Geodetic AN/USQ-28, Tenth Congress of the International Society of Photogrammetry, Lisbon, Portugal, September 15, 1964.

2. Range-Only Multiple Aircraft Navigation System, RADC-TR-72-22 dated February 1972, IBM, Rome Air Development, Center, Griffiss AFB NY. (AD 738696)

3. Final Survey Data, Rome Air Development Center, MINI-ELS Instrumentation Sites, Griffiss AFB NY, Geodetic Survey F. E. Warren AFB WY, July 1977.

APPENDIX A

DISTANCE MEASUREMENT EQUIPMENT (DME) NAVIGATION

This appendix describes one kind of ground-air Distance Measurement Equipment (DME) Navigation System, using pulsed data, that meets the precision required for extension of geodetic position. In addition to determining accurate position and derivatives of position, the link transmits data, includes error correcting codes (Hanning-Reed Solomon), and is a full duplex system operating at L band.

Figure A-1 is a simplified diagram showing the basic airborne portion of the Distance Measurement Equipment and the ground station. A master navigation computer is located at a Ground Control Station and contains a Kalman filter implementation that performs A/C to grid, coordinate transfer, performs integration of measurements, does pre-filtering of airborne measurements (when air derived sensors are used) and bias error correction. The transmitted messages that includes a ranging pulse are made up of 8 words extending over 500 usecs. Each word consists of a preamble, eight triple pulses and a ranging pulse at the end of the sequence. Figure A-2 illustrates the format of transmitted information. The initiation of the Radio Frequency (RF) transmission sets a clock at the DME Ground Control Station (GCS) and the reception of the signal at aircraft and from the DME GCS through the aircraft to ground beacon stations sets clocks at these locations. The range is determined by comparing clock times. These clock times obtained from various transmission paths are converted to range values in the DME GCS navigation computer.

Simplified transmission paths for a GCS and two remote beacon/transponder configurations are shown in Figure A-3. Path 1 is from the GCS to Aircraft No. 1, through the airborne hardware, calibrates the equipment delays, initiates the aircraft clock and retransmits to the GCS. Path 2 goes to the Aircraft No. 1 and is redirected to Remote Beacon 1 where the beacon hardware delays are calibrated, the beacon clock is reset and the message is retransmitted to the GCS through the Aircraft No. 1. The range measurement is, therefore, the round trip path from the Beacon No. 1 to the Aircraft No. 1 and hence to the GCS. The sequence to obtain calibration of hardware delays, send messages to three aircraft and two ground beacons, position location requires transmission times on the order of 4 milliseconds.

The random error in range is determined by referencing time to the half power point on the leading edge of the last pulse in the message sequence in Figure A-2. The variance in a single observation is directly related to the slope of the leading edge and inversely proportional to the square root of the signal energy to noise power and the number of single observations processed prior to a range determination. Single range observations are made at the rate of 30 per second. Ten measurements are integrated prior to a range readout. Random errors in time determination on a single observation are on the order of 10-15 nanoseconds for 20 dB signal-to-noise ratio. Residual bias errors are 7-15 nanoseconds. Certain error sources affecting the random and systematic errors have corrections applied.

Multiple path effects are eliminated by correlating Triplets received with known message structure. Standard corrections are made

for propagation. Angles of transmission are normally high virtually illuminating residual propagation errors, and the frequency of operation is optimum with regard to environmental noise. Major component of noise is the electronic equipment and variation in signal energy due to range dependent (R^2) loss and nulls in antenna patterns.

A simplified diagram of the computational process is shown in Figure A-4. Computation is done at the GCS. Computation includes the co-variance matrices and Kalman filter states for each aircraft. Serial processing is performed on the navigation data. The navigation data includes three position, velocity and acceleration for each aircraft referenced to the geocentric inertial frame. Computation is done in the aircraft frame of reference (DME information is also transformed into the platform frame). The Kalman filter has twelve states as initial conditions; they are 3 axis inertial platform misalignment, 3 aircraft position states, 3 aircraft velocity states and 3 inertial platform gyro states. Only the x, y, z, $\dot{x}$, $\dot{y}$, $\dot{z}$ for three aircraft are of concern; therefore, the navigation and measurement error co-variance matrices are 18 x 18. Data on the effectiveness in reducing range and velocity errors through complimentary filtering has yet to be obtained.

Emphasis is on improving aircraft velocity rather than position. Therefore, position measurement originally submitted should be used until measurements confirm a change is warranted. Of course, Kalman filtering cannot reduce bias error.

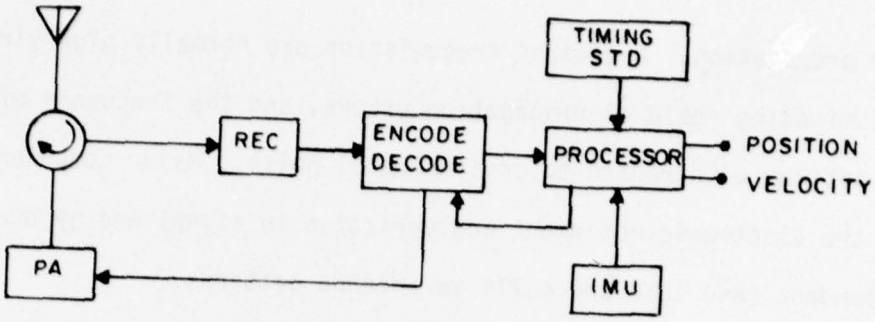

AIRCRAFT

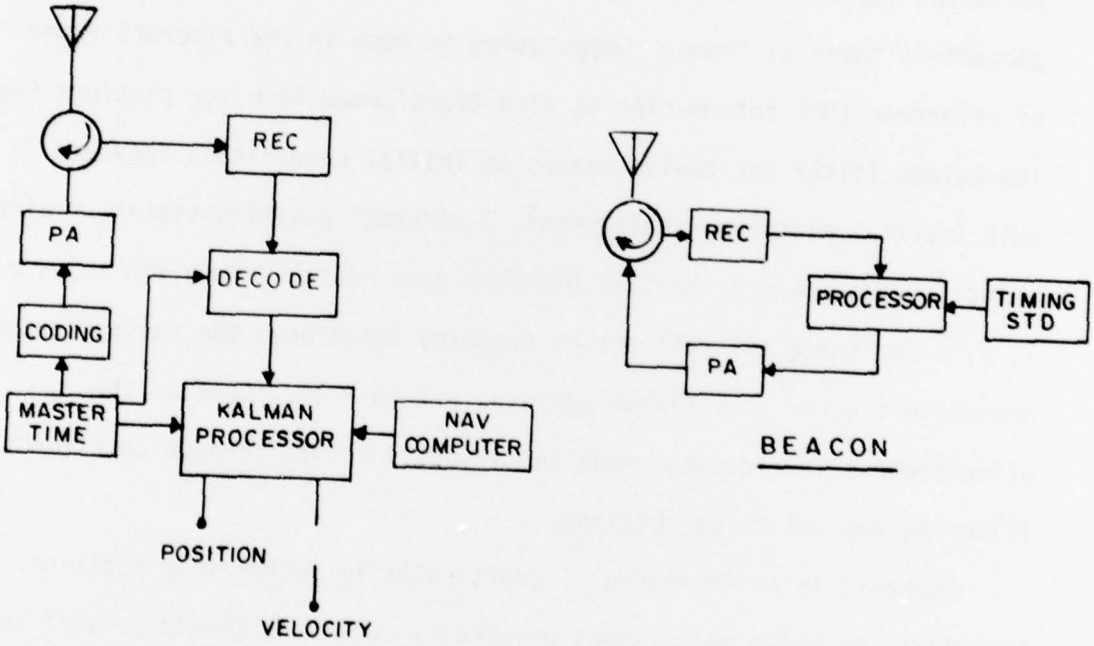

GROUND CONTROL STATION

BEACON

TYPICAL FUNCTIONAL BLOCK DIAGRAM
DISTANCE MEASUREMENT EQUIPMENT (DME) &
NAVIGATION

FIG. A-1

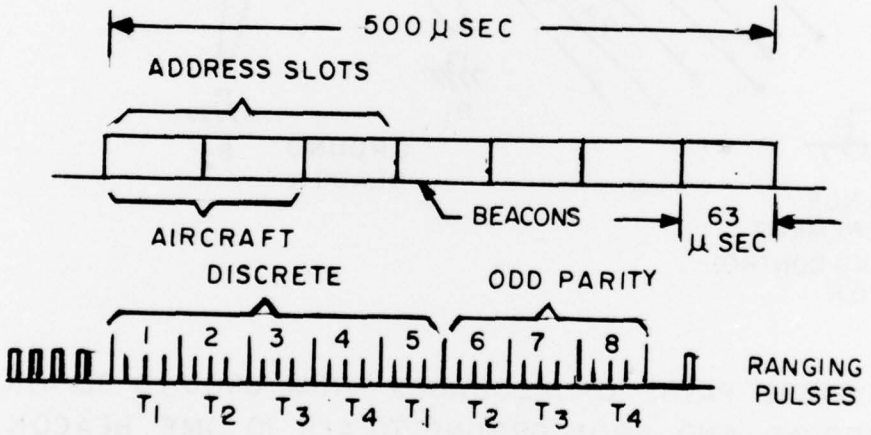

MESSAGE STREAM TO ONE AIRCRAFT

FIG. A-2

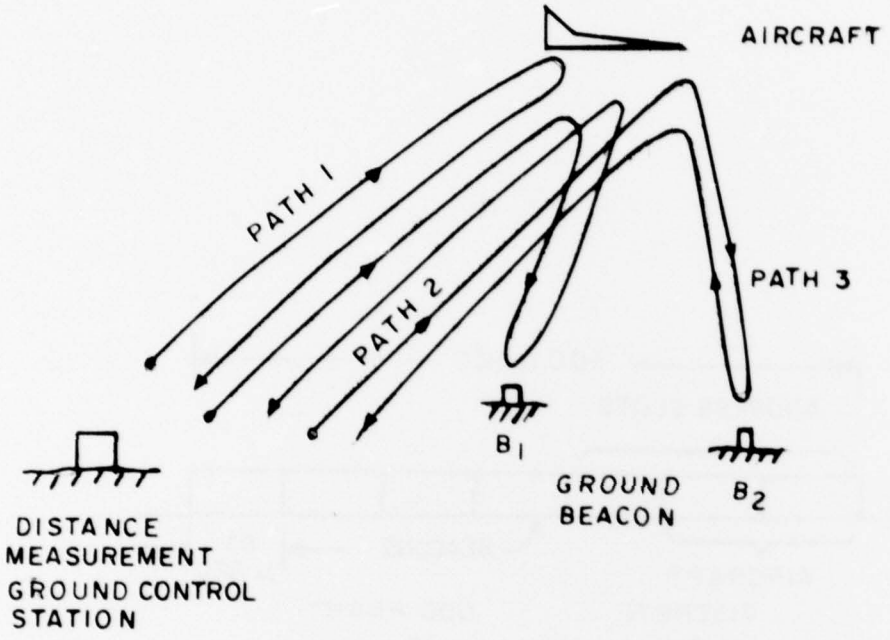

TYPICAL PATHS OF MESSAGES FROM GROUND TO AIR & GROUND AND FROM GROUND TO AIR TO DME BEACON AND RETURN

FIG. A-3

APPENDIX B

GENERAL PHOTOGRAMMETRIC BUNDLE ADJUSTMENT SOLUTION

1. Introduction

The procedure to be employed is a simultaneous photogrammetric bundle adjustment solution. All computations concerning photo (sensor) orientation and position, DME control coordinates, photo coordinates and added parameters are handled with a unified approach. It is defined as the least square solution for all unknown parameters using all of the image and DME Navigation Range coordinate observations for the photos in question. This procedure is highly flexible as it can be applied to photographs, digital records, blocks of photography, etc. The actual degree of flexibility will obviously be constrained by the cost-effectiveness of the computations.

The following discussion briefly describes the general photogrammetric bundle adjustment solution (simultaneous record adjustment). Paragraph 2 covers the basic condition equation. The linearized condition is given in Paragraph 3. General and special solutions are discussed in Paragraph 4.

2. Basic Condition Equation

The collinearity equation is the basic condition equation which relates the DME range coordinates to the photo coordinates. This equation type is the basis for single photo resection, relative orientation and strip or block aerotriangulation.

Collinearity Equations - Basically ground (DME Navigation Range) coordinates are related to photo coordinates in these equations.

$$x_{ij} - dx_{ij} = -C_i \frac{A1}{A3}$$
$$y_{ij} - dy_{ij} = -C_i \frac{A2}{A3} \qquad (1)$$

where

$$\begin{bmatrix} A_1 \\ A_2 \\ A_3 \end{bmatrix} = M_i \begin{bmatrix} X_j - X_i^c \\ Y_j - Y_i^c \\ Z_j - Z_i^c \end{bmatrix} \qquad (2)$$

Equation terms are

C_i - principal distance for i-th photo.

x_{ij}, y_{ij} - photo coordinates for j-th point of i-th photo.

dx_{ij}, dy_{ij} - distortions to ij-th image because of any added parameters

M_i - orthogonal rotation matrix for i-th photo.

$$M_i = \begin{bmatrix} C\emptyset CK & : & CWSK + SWS\emptyset CK & : & SWSK - SWS\emptyset CK \\ -C\emptyset CK & : & CWCK - SWS\emptyset SK & : & SWCK + CWS\emptyset SK \\ S\emptyset & : & -SWC\emptyset & : & CWC\emptyset \end{bmatrix} \qquad (3)$$

where $C\emptyset$ = cos phi; SK = sin kappa; CW = cos omega; etc. Omega, phi and kappa are primary, secondary and tertiary rotations.

X_j, Y_j, Z_j - ground coordinates of j-th point.

X_i^c, Y_i^c, Z_i^c - ground coordinates of camera station for i-th photo.

3. Linearized Conditions

The basic collinearity condition is nonlinear. Since most solutions will use a least squares adjustment and these computations are generally performed with linear functions, it is necessary to linearize the basic conditions. Series expansions, and Taylor Series in particular, are generally used for this process where only the zero and first-order terms are included.

The linearized expression for the collinearity equations can be presented in matrix notation as follows:

$$\underset{(a,1)}{v_{ij}} + \underset{(a,b)(b,1)}{\overset{o}{B}_{ij}\ \overset{o}{S}_{ij}} + \underset{(a,c)(c,1)}{\overset{\rho}{B}_{ij}\ \overset{\rho}{S}} + \underset{(a,3)(3,1)}{\overset{G}{B}_{ij}\ \overset{G}{S}_{j}} + \underset{(a,1)}{\varepsilon_{ij}} = 0 \qquad (4)$$

where

v_{ij} = vector of residuals for the observation of the ij-th image.

$\overset{o}{B}_{ij}$ = matrix of partial derivatives for the orientation parameters of the i-th unit.

$\overset{\rho}{B}_{ij}$ = matrix of linear coefficients for the added parameters.

$\overset{G}{B}_{ij}$ = matrix of partial derivatives for the ground coordinates of the j-th point.

$\overset{o}{S}_{i}$ = vector of corrections for the orientation parameters of the i-th unit.

$\overset{\rho}{S}$ = vector of added parameters.

$\overset{G}{S}_{j}$ = vector of corrections for the ground coordinates of the j-th point.

ε_{ij} = discrepancy vector for the ij-th image.

a = number of observation equations per photogrammetric point that is observed. (2 for photos - x,y coordinates)

b = number of orientation parameters per unit (6 for each photo).

c = number of added parameters.

If "a priori" values are available for the orientation parameters, added parameters, or ground coordinates they can be treated as observations as follows:

$$\underset{(b,1)}{v_i^o} - \underset{(b,1)}{s_i^o} + \underset{(b,1)}{\varepsilon_i} = 0 \text{ (orientation parameters of the i-th unit)} \quad (5)$$

$$\underset{(c,1)}{v^\rho} - \underset{(c,1)}{s^\rho} + \underset{(c,1)}{\varepsilon^\rho} = 0 \text{ (added parameters)} \quad (6)$$

$$\underset{(3,1)}{v_j^G} - \underset{(3,1)}{s_j^G} + \underset{(3,1)}{\varepsilon_j^G} = 0 \text{ (ground coordinates of the j-th point)} \quad (7)$$

where

v_i^o, v^ρ, v_j^G = vectors of residuals for the observations.

ε_i^o, ε^ρ, ε_j^G = discrepancy vectors for the observations.

The weight matrices for the observations are:

w_{ij} = image observations

(a,a)

$\overset{o}{w}_i$ = orientation parameters

(b,b)

$\overset{\rho}{w}$ = added parameters

(c,c)

$\overset{G}{w}_j$ = ground coordinates

(3,3)

4. General or Special Solutions

The completely general solution would allow for the simultaneous solution of equation types (4), (5), (6) and (7). Special solutions would allow for all combinations of the above equation types. The weight matrices would be used as constraints allowing various parameters to be treated as known or unknown.

As an example, suppose a stereo pair were being evaluated and there were ten points of interest in the stereo model. Of these ten points, the ground coordinates were known for 4 of them. The orientation parameters for each photo are unknown, 5 added lens distortion parameters are unknown and the X, Y, Z coordinates of six of the object points are unknown. For this solution, the following 2 types of linearized observation equations are to be used:

$$v_{ij} + \overset{o}{B}_{ij}\,\overset{o}{S}_i + \overset{\rho}{B}_{ij}\,\overset{\rho}{S} + \overset{G}{B}_{ij}\,\overset{G}{S}_j + \varepsilon_{ij} = 0 \qquad (8)$$

$$v_j^G - S_j^G + \varepsilon_j^G = 0 \qquad (9)$$

In this case "a priori" values are provided only for the ground coordinates of the four known points. All other unknowns will be approximated and weights of zero supplied in each case.

In this example, there will be 40 type (8) equations and 30 type (9) equations.

These 70 equations are expressed as follows:

$$\bar{v} + \bar{B}\,\bar{S} + \bar{\varepsilon} = 0 \qquad (10)$$

where

$$\bar{v} = \begin{bmatrix} v_{ij} \\ \\ v_j^G \end{bmatrix} \qquad B_S = \begin{bmatrix} B_{ij}^o & B_{ij}^\rho & B_{ij}^G \\ \\ 0 & 0 & -I \end{bmatrix}$$

$$\bar{S} = \begin{bmatrix} S^o \\ \\ S^\rho \\ \\ S^G \end{bmatrix} \qquad \bar{\varepsilon} = \begin{bmatrix} \varepsilon_{ij} \\ \\ \varepsilon^G \end{bmatrix}$$

The reduced normal equations will be of rank (6 x m + 3 x n + c) where m equals the number of photos, n equals the number of ground points and c equals the number of added parameters. For the given example there will be [(6x2) + (3x10) + 5 = 47] normal equations, one for each unknown. The 70 observation equations are now reduced to the 47 normal equations which are symbolized as follows:

$$\underset{(47,47)}{\overline{N}} \quad \underset{(47,1)}{\overline{S}} \quad + \quad \underset{(47,1)}{\overline{C}} \quad = \quad 0 \tag{11}$$

where

$$\overline{N} = \overline{B}^{T}\,\overline{W}\,\overline{B}\;;\quad \overline{C} = \overline{B}^{T}\,\overline{W}\,\overline{\varepsilon}\;;\quad \overline{W} = \begin{bmatrix} W & 0 & 0 \\ 0 & W^{\rho} & 0 \\ 0 & 0 & W^{G} \end{bmatrix}$$

The solution for corrections to first approximations would be calculated as follows:

$$\overline{S} = -\overline{N}^{-1}\,\overline{C} \tag{12}$$

The $\overline{S}$ quantities would be added to the first approximations and sufficient iterations processed for the sum of the weighted residuals squared to become a minimum ($\overline{V}^{T}\,\overline{W}\,\overline{V} \rightarrow$ minimum). Thus, the best estimates for the unknowns, 47 in this case, are obtained.

The precision of each calculated unknown is obtained as a by product of the least squares solution.

$$\text{Covariance matrix } (\Sigma) = q_{ij} = \hat{\sigma}_o^2 \, \bar{N}^{-1} \tag{13}$$

where

$$\hat{\sigma}_o^2 = \frac{\bar{V}^T \bar{W} \bar{V}}{\gamma}$$

$$\bar{V} = -\bar{\varepsilon}$$

γ = number of degrees of freedom which is 23 in the preceding example.

The standard deviations of the unknowns are the square roots of the diagonal terms of the covariance matrix.

The general solution as modified by weight constraints can be used in many combinations, one of which has been used as an example.

MISSION
of
Rome Air Development Center

RADC plans and executes research, development, test and selected acquisition programs in support of Command, Control Communications and Intelligence (C^3I) activities. Technical and engineering support within areas of technical competence is provided to ESD Program Offices (POs) and other ESD elements. The principal technical mission areas are communications, electromagnetic guidance and control, surveillance of ground and aerospace objects, intelligence data collection and handling, information system technology, ionospheric propagation, solid state sciences, microwave physics and electronic reliability, maintainability and compatibility.